

**OPTICAL AND ELECTRICAL CHARACTERIZATION OF $Cd_xSe_{1-x}S$ AND
 Cu_2S THIN FILMS FOR SOLAR CELL APPLICATION**

MOGUNDE CHARLES MORARO (B.EdSc)

I56/CE/22416/2010

A thesis submitted in partial fulfillment of the requirement for the award of the Degree of Masters of Science (Electronics and Instrumentation) in the School of Pure and Applied Sciences of Kenyatta University.

December, 2016

DECLARATION

This thesis is my original work and has not been presented for a degree in any other University or any other award.

Mogunde Charles Moraro Signature.....Date.....

Department of Physics

Kenyatta University

I/We confirm that the work reported in this thesis was carried out by the student under my/our supervision.

Supervisors

Dr. Walter K. Njoroge

Signature.....Date.....

Department of Physics

Kenyatta University

Dr. Mathew K. Munji

Signature.....Date.....

Department of Physics

Kenyatta University

DEDICATION

I dedicate this thesis to my parents, wife and children for their endless love, support and encouragement.

ACKNOWLEDGEMENT

Foremost, I thank God for the good health and the opportunity to accomplish my research against all challenges. Thanks to Kenyatta University for the study opportunity.

I would like to sincerely thank my supervisors, Dr. Walter Njoroge and Dr. Mathew Munji for their valued comments, opinions and suggestions throughout this study. Special thanks to Dr. Sebastian Waita of University of Nairobi whose wealth of knowledge in deposition of thin films by solution techniques inspired me to pursue my research to the end. I also recognize the Physics Department lecturers who patiently guided me through their recommendations, constructive discussions during research.

With great pleasure, I thank The National Commission for Science, Technology and Innovation (NACOSTI) for funding my research. I give special appreciation to University of Nairobi, Chiromo campus for allowing me to use some of the equipment donated by Uppsala University for research. I thank the technical staff in Kenyatta University and University of Nairobi for technical assistance during my research.

To all my family members and friends, I thank you for all manner of support you gave me throughout my research. I cannot list all the names here, but you will always be in my mind.

TABLE OF CONTENTS

DECLARATION.....	ii
DEDICATION	iii
ACKNOWLEDGEMENT	iv
LIST OF TABLES	ix
LIST OF FIGURES	x
ABBREVIATIONS	xii
SYMBOLS	xiv
ABSTRACT	xvi
CHAPTER 1.....	1
INTRODUCTION	1
1.1 Introduction	1
1.2 Background of the study	1
1.3 Materials and components.....	1
1.4 Statement of the research problem	3
1.5 Objectives.....	3
1.5.1 General objective	3
1.5.2 Specific objectives	3
1.6 Rationale of the study	4
CHAPTER 2.....	6
LITERATURE REVIEW	6
2.1 Introduction	6
2.2 Development of solar cells.....	6
2.3 Review of thin films and solar cells fabricated	8
2.3.1 Copper (I) sulphide	8
2.3.2 Cadmium Selenide doped with Indium and Silver	9
2.3.3 CdS doped with chlorine, lead and cobalt.....	10
2.3.4 CdSe/Cu ₂ S and CdS/Cu ₂ S solar cells.....	11
2.4 Improving optical and electrical properties of CdSeS/Cu ₂ S solar cells.....	11
CHAPTER 3.....	13
THEORY OF THIN FILMS AND P-N JUNCTION.....	13

3.1 Introduction	13
3.2 Semiconductor thin films	13
3.3. The p-n Junction	13
3.4 Photovoltaic effect and solar cells	15
3.5 Energy band gaps in semiconductors.....	16
3.6 Intrinsic carrier concentration and fermi energies.....	18
3.7 Doping of semiconductors	19
3.8 Current conduction in semiconductors	20
3.8.1 Intrinsic charge carriers	20
3.8.2 Extrinsic charge carriers	20
3.8.3 Drift current (Mobility)	22
3.8.4 Influence of applied electric field on charge carriers.....	23
3.8.5 Diffusion current.....	24
3.9 Types of band gaps	24
3.9.1 Direct band gap semiconductors.....	25
3.9.2 Indirect band gap semiconductors	26
3.10 Thin film applications	26
3.11 Performance of a solar cell.....	27
3.11.1 Light trapping	27
3.11.2 Solar cell parameters	27
3.11.3 Solar cell conversion efficiency.....	29
3.12 Conversion efficiency limits	30
3.12.1 Spectral mismatch	30
3.12.2 Reflectance	30
3.12.3 Shading losses.....	30
3.12.4 Absorption loss	30
3.12.5 Collection losses	31
3.12.6 Recombination and series resistance.....	31
CHAPTER 4.....	32
EXPERIMENTAL PROCEDURES	32
4.1 Introduction	32

4.2 Materials for thin film deposition	32
4.2.1 Deposition of p-type Cu_2S thin films.....	32
4.2.2 Deposition of CdSeS	32
4.3 Cleaning of the glass substrates.....	33
4.4 Experimental set-up	33
4.5 Procedure.....	34
4.5.1 Deposition of Cadmium Seleno-sulphate thin films.....	34
4.5.2 Deposition of copper (I) sulphide Cu_2S thin films	35
4.6 Characterization of thin films procedures.....	36
4.6.1 Optical characterization of thin films.....	36
4.7.2: Electrical properties	38
4.8 Fabrication of the $\text{Cd}_x\text{Se}_{1-x}\text{S}/\text{Cu}_2\text{S}$ solar cell.....	39
4.9 Characterization of solar cell.....	39
CHAPTER 5.....	41
RESULTS AND DISCUSSION	41
5.1 Introduction	41
5.2 Optical properties of p-type Cu_2S	41
5.2.1 Transmittance	41
5.2.2 Reflectance	42
5.2.3 Absorbance	43
5.2.4 Refractive index (n)	44
5.2.5 Band gap.....	45
5.2.6 Absorption coefficient.....	47
5.3. Electrical Properties of p-type Cu_2S	48
5.4 Optical properties of CdSeS	51
5.4.1 Transmission.....	51
5.4.2 Absorbance	51
5.4.3 Reflectance	51
5.4.4 Extinction coefficients (k).....	52
5.4.5 Absorption coefficient of CdSeS	53
5.4.6 Refractive index of CdSeS	55

5.4.7 Di-electric constant of CdSeS.....	56
5.4.8 Optical energy band gap of CdSeS	57
5.5 Electrical Properties of CdSeS	59
5.6 Optimized opto-electric properties for solar cell application.....	62
5.6.1 n-type window layer.....	62
5.6.2 P-type absorption layer.....	63
5.7 Solar cell I-V Characteristics	63
5.8 Solar cell fill factor (FF) and conversion efficiency (η)	63
CHAPTER 6.....	67
CONCLUSIONS AND RECOMMENDATIONS.....	67
6.1 Conclusions	67
6.2 Recommendations.....	68

LIST OF TABLES

Table 4.1: Composition of Bath constituents for preparing CdSeS.....	34
Table 4.2: Composition of reagents used to deposit Cu ₂ S thin films.....	35
Table 5.1: Energy gaps of Cu ₂ S thin films of different thickness.....	47
Table 5.2: Absorption coefficients of Cu ₂ S of different wavelengths.....	47
Table 5.3: Electrical properties of p-type Cu ₂ S.....	49
Table 5.4: Summary of optical and electrical characteristics of Cu ₂ S thin films.....	50
Table 5.5: Energy gaps of CdSeS thin films of different thickness.....	58
Table 5.6: Electrical properties of CdSeS.....	59
Table 5.7: Summary of Opto-electric properties.....	62
Table 5.8: The I-V characteristics of the CdSeS/Cu ₂ S solar cell under illumination	64

LIST OF FIGURES

Figure 1.1 Typical structure of a solar cell.....	2
Figure 2.1 The Graph of development of solar cells from 1975 up to 2015.....	7
Figure 3.1 A typical p-n junction.....	14
Figure 3.2 A p-n hetero-junction.....	15
Figure 3.3 Energy band diagram of a p-n junction showing the location of carriers under zero voltage bias.....	16
Figure 3.4 Conduction and Valence bands of a typical semiconductor.....	17
Figure 3.5 Bonding in Si lattice with Boron and phosphorus.....	20
Figure 3.6 E-k Diagram of a direct band gap semiconductor.....	25
Figure 3.7 E-k Diagram of indirect band gap semiconductors.....	26
Figure 3.8 Reflection coefficient of a polished and ARC coated silicon surfaces.....	28
Figure 3.9 The typical I-V characteristics of a solar cell.....	29
Figure 4.1 Chemical bath Deposition set-up.....	33
Figure 4.2 Spectrum Analyzer.....	36
Figure 4.3 Schematic cross-section of a solar cell.....	39
Figure 5.1: Transmission spectra of Cu ₂ S thin films.....	41
Figure 5.2: Reflectance spectra of Cu ₂ S thin films.....	43

Figure 5.3: Absorbance spectra of Cu ₂ S thin films.....	44
Figure 5.4: Refractive index of Cu ₂ S thin films.....	45
Figure 5.5: Absorption coefficient of Cu ₂ S of different photon energies	46
Figure 5.6: Absorption coefficient of Cu ₂ S versus wavelength.....	48
Figure 5.7: Electrical resistivity and conductivity varied with concentration of Cu ²⁺ ions.....	50
Figure 5.8: Transmission spectra of CdSeS thin films.....	52
Figure 5.9: Absorbance spectra of CdSeS thin films.....	53
Figure 5.10 Reflectance spectra of CdSeS thin films.....	54
Figure 5.11: A plot of extinction coefficient of CdSeS thin films.....	54
Figure 5.12: Absorption coefficient of CdSeS thin films.....	55
Figure 5.13: Refractive index of CdSeS thin films.....	56
Figure 5.14: A plot of real di-electric constant against wavelength.....	57
Figure 5.15: Energy band gap determination.....	58
Figure 5.16: A graph of resistivity against thin film thickness of CdSeS.....	60
Figure 5.17: Optimization of resistivity of CdSeS thin films.....	61
Figure 5.18: Plot of I-V characteristics of a solar cell.....	65

ABBREVIATIONS

A_c	Area of a cell
AM	Air Mass
CB	Conduction band
CBD	Chemical Bath Deposition
CVD	Chemical Vapour Deposition
E_c	Conduction band Energy
eV	Electron volt
E_v	Valence band Energy
FF	Fill factor
HVE	High Vacuum Evaporation
ITO	Indium Tin Oxide
I-V	Current verses Voltage
NIR	Near Infra-red spectroscopy
PVD	Physical Vapour Deposition
P_{IN}	Power in
P_{MAX}	Maximum Power
P_{OUT}	Power Out
TCO	Transparent Conducting Oxide
UV	Ultra-Violet

VB	Valence band
VIS	Visible
V_{oc}	Open circuit voltage

SYMBOLS

Ag	Silver
c	Speed of radiation
CdS	Cadmium Sulphide
CdSe	Cadmium Selenide
Cd _x Se _{1-x} S	Cadmium Seleno-sulphide
Cu ₂ S	Copper (I) Sulphide
E	Irradiance of light
E _g	Band gap Energy
h	Planck's constant
I ₀	Intensity of incident photon
I _{sc}	Short-circuit current
K _B	Boltzman constant
k	Extinction coefficient
q	Elementary charge
T ₀	Absolute temperature
α	Absorption coefficient
ε	Dielectric constant
η	Solar conversion efficiency
λ	Wavelength
π	pi

ρ	Electrical resistivity
σ_0	Optical conductance
Ω	Ohms
μ	Electron mobility
M	concentration of solution in moles per litre
n	Intrinsic/extrinsic high density electron concentration
n	Refractive index
p	Intrinsic/extrinsic high density hole concentration
p-n	The interface between p-type and n-type semiconductors
SnO ₂	Tin oxide

ABSTRACT

There has been a steady increase in demand for clean and renewable energy globally. As a result, more effort has been put into research to harness solar energy from the sun to generate electricity using solar cells. Solar cells convert solar energy directly into electricity. Recent research findings indicate that properties of thin film solar cells strongly depend on the various deposition techniques chemical bath deposition (CBD) being one of them. This technique yields stable, adherent, uniform and hard films with good reproducibility by a relatively simple process. In this research, CBD method was used to deposit thin films of cadmium seleno-sulphide ($\text{Cd}_x\text{Se}_{1-x}\text{S}$) and Copper (I) sulphide (Cu_2S) on glass substrates. Solutions of copper (II) sulphate, thiourea and tartaric acid were used to deposit Cu_2S thin films at constant temperature $40 \pm 2^\circ\text{C}$ whereas solutions of cadmium nitrate, thiourea and Sodium Seleno-sulphate were used to deposit $\text{Cd}_x\text{Se}_{1-x}\text{S}$ thin films at constant temperature of $60 \pm 2^\circ\text{C}$. The optoelectronic properties of both films were investigated. Electrical properties like sheet resistivity (ρ) were investigated using a four point probe connected to a Keithley 2400 source meter interfaced with computer. The electrical resistivity of Cu_2S decreased from $479 \Omega/\square$ to $87 \Omega/\square$ with increasing concentration of copper (II) ions. Resistivity of cadmium seleno-sulphate thin films decreased from $175.54 \Omega/\square$ to $130.78 \Omega/\square$ with increase of selenium concentration. Optical properties like reflectance and transmittance were determined using UV-VIS NIR 3700 spectrophotometer in the range of wavelength between 300-1200 nm. Transmittance of Cu_2S thin films varied between 10 and 40% with wavelength of the light energy whereas that of CdSeS varied between 75 and 87%. Transmittance and reflectance were simulated by scout software from which other optical parameters like band gap (E_g), refractive index (n), extinction coefficient (k) and absorption coefficients (α) were calculated. The plots of $(\alpha hv)^2$ against hv were used to determine energy gaps (E_g) of Cu_2S and CdSeS thin films. Energy gaps of Cu_2S varied between 1.68eV to 2.64eV and that of $\text{Cd}_x\text{Se}_{1-x}\text{S}$ thin films varied from 2.64eV to 3.314eV. The copper (I) sulphide thin film with optimum properties of an active part of a solar cell was selected. The CdSeS with optimum window layer optoelectric characteristics was selected. Optimized parameters comprised electrolyte pH, bath temperature and concentrations of cadmium and copper ions in the n and p type materials respectively. The fabricated solar cell was characterized by solar cell simulator. The solar cell's diode characteristics like short circuit current ($I_{sc} = 0.0039\text{A}$), open voltage ($V_{oc} = 0.40\text{V}$), fill factor ($\text{FF} = 0.60$) and conversion efficiency ($\eta = 0.81\%$) were obtained. The characteristics obtained shows that the solar cell materials used have properties that can be enhanced to fabricate commercial solar cells.

CHAPTER 1

INTRODUCTION

1.1 Introduction

This chapter presents the background of the study, materials and components, statement of the research problem, objectives, and rationale of the study and lastly the structure of the thesis.

1.2 Background of the study

Solar cells are the smallest devices that can be used as irradiance sensors or as samples for studying new solar materials (Misle, 2009). Photons absorbed by the solar cells are converted to electrical power (Mohammed *et al.*, 2007). According to Boyle (1996) energy from the sun is relatively clean and reliable than gas, coal, and oil. Solar energy is significantly abundant and pollution free (Nault, 2005). Thin film technology is utilized to fabricate solar cells that produce power for domestic and commercial uses. Solar energy system is reliable, easy to maintain and install (Siu and Kwok, 1978; Armin, 2009).

1.3 Materials and components

Figure 1.1 shows the primary features of silicon solar cell. A solar cell consists of a p and n type layers that enable current to flow as electron-hole pairs are created (Kassim *et al.*, 2010).

Semiconductor thin films form part of window and absorber materials of a solar cell. A p-type absorber layer of thickness of about 300 μm lies beneath n-type window layer. The n-type layer on top side is more transparent and less thick than p-type. Doping the layers help to separate charge carriers.

Solar cells consist of metallic electrical contacts that collect the separated charge carriers. The electrical contacts connect the cell to an external load. An antireflection coating (ARC) covers the top side of the cell so as to reduce the reflection of light from the cell and to shield the solar cell against the environmental effects that cause degradation.

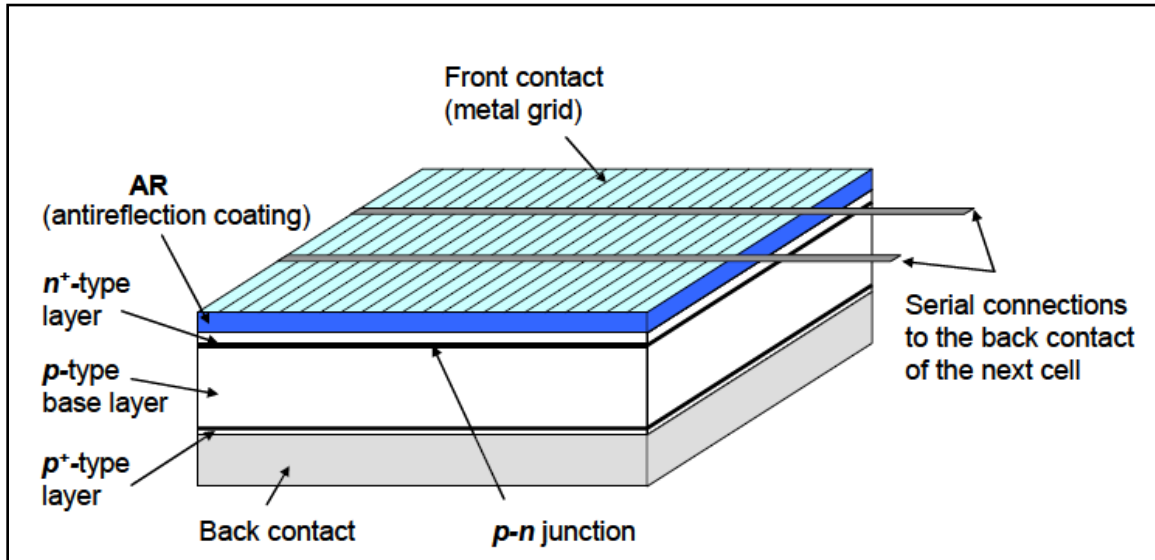


Figure 1.1 typical structure of a solar cell (Zeman, 2003)

Metal chalcogenides (binary elements) such as CdS and CdSe when doped, form desirable window material properties (Khallaf *et al.*, 2009; Fatehmulla *et al.*, 2014). Ternary thin films have generated a lot of research interest for solar cell applications. $\text{Cd}_{1-x}\text{Se}_x\text{S}$ is a candidate for wide band gap material for solar cell applications. Desirable qualities of $\text{Cd}_x\text{Se}_{1-x}\text{S}$ and Cu_2S thin films for solar cell fabrication can be obtained by chemical bath deposition method. Optimizing factors like the reaction bath temperature, electrolyte pH, concentration of the reactants and complexing agents, nature of substrates, duration of the reaction and annealing influence the cell efficiency. These factors need to be studied.

1.4 Statement of the research problem

There is need to study and look for the best materials for fabrication of solar cells that convert efficiently solar energy to electrical power. There is limited information on cadmium seleno-sulphide ($\text{Cd}_x\text{Se}_{1-x}\text{S}$) and copper (I) sulphide (Cu_2S) thin films for solar cell applications. This study was aimed at investigating both the optical and electrical properties of $\text{Cd}_x\text{Se}_{1-x}\text{S}$ and Cu_2S thin films using chemical bath deposition (CBD) method. In addition to investigation of the opto-electric properties, this study was aimed at improving these properties as well as to provide additional information on the $\text{Cd}_x\text{Se}_{1-x}\text{S}/\text{Cu}_2\text{S}$ solar cell.

1.5 Objectives

1.5.1 General objective

To optically and electrically characterize $\text{Cd}_x\text{Se}_{1-x}\text{S}$ and Cu_2S *p-n* junction for solar cell application.

1.5.2 Specific objectives

- i) To deposit $\text{Cd}_x\text{Se}_{1-x}\text{S}$ and Cu_2S thin films by Chemical Bath Deposition method.
- ii) To investigate electrical properties of $\text{Cd}_x\text{Se}_{1-x}\text{S}$ and Cu_2S thin films by four point probe method.
- iii) To determine the optical properties of $\text{Cd}_x\text{Se}_{1-x}\text{S}$ and Cu_2S thin films using a spectrophotometer in the range between 300-1200 nm.
- iv) To fabricate and characterize $\text{Cd}_x\text{Se}_{1-x}\text{S}/\text{Cu}_2\text{S}$ solar cell using a solar cell simulator.

1.6 Rationale of the study

Ternary semiconductor thin films are known to have suitable properties for solar cell applications among them is a well-defined band structure (Omar, 1975). The composition of their constituent elements influences the energy gap values (Fatehmulla *et al.*, 2014). Ternary semiconductor thin films have direct band gaps necessary for the fabrication of solar cells. $Cd_xSe_{1-x}S$ is one such ternary semiconductor that can be used to fabricate solar cells. There is little research that has been reported on the use of $Cd_xSe_{1-x}S$ and Cu_2S materials for solar cell application. This work intends to use $Cd_xSe_{1-x}S$ as window material and Cu_2S as an absorber material in the fabrication of a solar cell because there is little information on their use.

1.7 Structure of the thesis

This thesis is structured into six chapters.

Chapter 1 gives an introduction into the background of the research, the typical semiconductor solar cell structure, statement of the research problem, objectives and the rationale of the study. This chapter describes how a solar cell generates electric power and justifies the choice of suitable materials and methods for fabrication of a solar cell in consideration.

Chapter 2 covers the literature review of the semiconductor n-type materials like CdSe, CdS doped with In, Co, Ag and indium to improve opto-electric properties of thin films. p-type Cu_2S thin films are also explained.

Chapter 3 explains the theory of semiconductor thin films, their electrical and optical properties and their applications in solar cell fabrication. The chapter discusses the energy conversion efficiency and limitations of the solar cells.

Chapter 4 focuses specifically on the experimental procedures for deposition and fabrication of the solar cell under investigation- CdSeS/Cu₂S. The method of deposition is explained by help of Tables, figures and theory. The chapter also discusses the equipment and procedure used to investigate optical and electrical properties of solar cells.

Chapter 5 provides the results obtained from investigation of optical and electrical properties CdSeS and Cu₂S thin films. Results of optical properties like transmittance, reflectance, absorbance and optical constants of both films are reported in Tables, figures and graphs. The analyzed data is compared with the existing research appropriately.

Chapter 6 gives the conclusions and recommendations. This chapter closes with references cited.

CHAPTER 2

LITERATURE REVIEW

2.1 Introduction

In this chapter, literature review of related work on the deposition of various thin films for photovoltaic applications is done. Development of solar cells in terms of efficiency from 1992 to 2015 is illustrated graphically. Review of properties of copper (I) sulphide and cadmium selenide thin films doped with silver, indium and cobalt are discussed.

2.2 Development of solar cells

Energy demand has grown tremendously and this calls for research into harvesting eco-friendly and renewable sources. Among the potential sources is solar energy which is made available by solar cells (<http://www.bp.com>). The total amount of solar energy received by earth each second is about 1.74×10^{17} W, which is about 1.2×10^4 times more than the average world energy consumption in 2008. If captured effectively, even a small fraction of this energy can meet the rapidly growing energy demand of the world (<http://www.bp.com>).

Commercially, CdTe solar cell efficiency had not exceeded 13% by 2013 (Fraunhofer, 2015). Crystalline silicon solar cells dominate global market by 92% while the multi-crystalline solar cells like CdS/Cu₂S takes about 8% of total production. The high cost of manufacturing crystalline silicon solar cells has resulted to development of new and cheap multi-crystalline thin film technology. Pathan *et al.* (2002) reported achievement of practical efficiencies of 16% and experimental efficiencies of 24% of various thin film solar cells like CdS/CdTe and CIS/CIGS. Saraf (2012) reported an efficiency of 10.9% obtained from a cheaper CdS/Cu₂S hetero-junction thin film solar cell. He reported energy gaps of 4.4eV and 2.65eV for CdS and Cu₂S respectively.

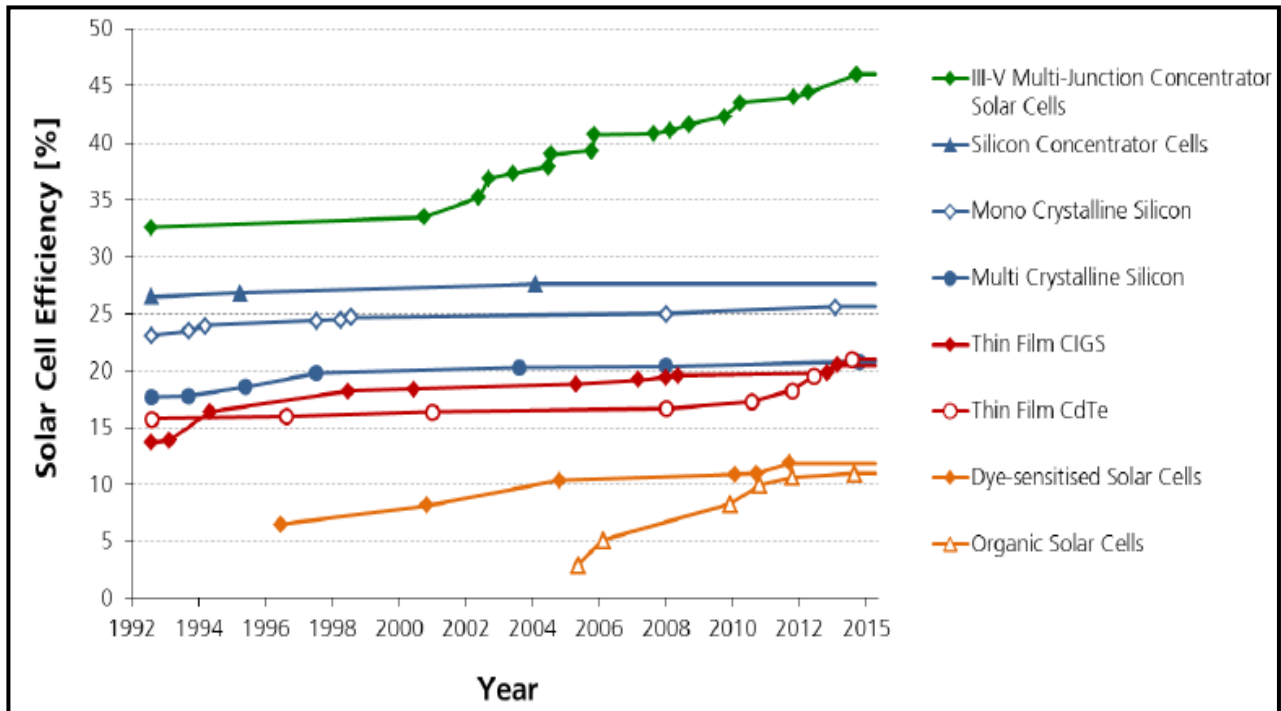


Figure 2.1 The development of solar cell fabrication from 1992 up to 2015(Philipps, 2015).

Crystalline silicon cells are somehow costly and have low mobility of charge. Therefore, semiconductor materials with superior charge carrier mobility and relatively low cost semiconductors are needed. Introduction of semiconductors like copper indium diselenide (CIS) and copper indium gallium diselenide (CIGS) have achieved laboratory efficiency of 18.8% due to the increase in effective band gap of 1.1 to 1.2 eV (Shah et al., 1999).

Gratzel (2003) reported that dye-sensitized solar cells achieved efficiency of approximately 10% in the laboratory. However, the electrolytic dye has challenges like the stability issues and additional costs for integrating into series connected systems.

Robert (2008) reported that nanocrystalline solar cells like PbSe generate two to three charge carriers per absorbed photon. Robert observed that preparing PbSe thin films from solution is

relatively cheaper than other commonly used methods. On the other hand, the efficiency measured was roughly 2.5% compared to the 44% theoretical value (Robert, 2008).

Energy delivered by the sun in one hour onto the earth can, if appropriately trapped, be utilized in one year (Doe, 2005). This supply surpasses all other energy sources. In the year 2000, BP Solarex developed two new thin film solar modules measuring 0.9 square meter that achieved 10.6 % conversion efficiency and a power output of 91.5 watts (<http://www.bp.com>). The modules produced were used to power the NASA's (The National Aeronautics and Space Administration) solar powered aircraft in 2001.

2.3 Review of thin films and solar cells fabricated

2.3.1 Copper (I) sulphide

Cu_2S thin film is a II-VI compound and is known to exist in several crystallographic and stoichiometric forms whose main advantage is for making low cost solar cells. In addition, it is easy to deposit and form good quality films from a variety of growth methods. (Maissel and Glang, 1970).

Wuet *al.* (2008) reported that 300 nm thick Cu_2S thin film prepared by solution process has a suitable band gap near 1eV for potential Photovoltaic application. When paired with CdS the photovoltaic device formed yielded power conversion efficiency of 1.6%.

Electrical resistivity of Cu_2S thin films results from the scattering of electrons by the lattice (Maissel and Glang, 1970). Normally resistivity of Cu_2S decreases for the film coated at higher thickness, which is due to increase in grain size of the film at higher thickness (Ramya and Ganesan, 2012). Refraction index of Cu_2S is proportional to the film thickness. Thin film of lower thickness has very low refractive index (Ramya, and Ganesan,

2012). The energy gap of Cu₂S thin film reported by Saadeldin *et al.* (2014) was 2.266 eV. It was a direct allowed transition. Similar results were reported by Mulder (2006). The thin film thickness varied from 111 nm to 453 nm and obtained direct band gap energies ranging from 2 eV to 2.5 eV.

Copper sulphide thin films have been greatly and extensively studied. These films show low reflectance below 10 % in the visible region. Thin films with low reflectance are used to minimize glare (Pathan *et al.*, 2002; Pathan and Lokhande, 2003).

Kassim *et al.* (2010) deposited CuS thin films on indium tin oxide by CBD technique at pH value of 3. The film was polycrystalline with hexagonal structure and had a p-type behavior. The band gap obtained was 2.6 eV.

2.3.2 Cadmium Selenide doped with Indium and Silver

Doping of CdSe with indium was done by Takanoglu *et al.* (2015) and observed that conductivity of CdSe increased with doping. Resistivity measurements of undoped CdSe thin film were $8.44 \times 10^4 \Omega/\square$ while the resistivity of a doped CdSe was $5.22 \Omega/\square$. Both measurements were done at room temperature. CdSe is a potential material for solar cell applications due to its high absorption coefficient and close to optimum direct energy gap.

Chalilha *et al.* (2008) doped CdSe with silver. The doped CdSe had lower resistivity than undoped CdSe because of possible change in structure, grain size and better crystallinity of a silver doped CdSe.

Doping of CdSe influences the energy band gap as reported. Energy gap is lowered as a result of increased free carriers and improvement of grain structure of thin films. Conversely, the energy band gap increases due to grain sizes becoming smaller. Smaller grain sizes can be explained by quantum confinement of electronic states in semiconductor material (Takanoglu *et al.*, 2015).

2.3.3 CdS doped with chlorine, lead and cobalt

Dharmadasa *et al.* (2014) fabricated CdS/CdTe thin films which absorbed UV, VIS and IR radiations and produced solar cell with efficiencies above 10%. It was found that doping CdS with Chlorine improved solar cell conversion efficiencies to about 16%. Chlorine as a dopant has also been investigated (Fatehmulla *et al.*, 2014). High Vacuum Evaporation (HVE) method was used to dope CdS films with chlorine by using a mixture of CdS and CdCl₂ powders at room temperature. Doping and annealing improved resistivity (ρ), carrier concentration (n) and mobility (μ) of CdS:Cl films. Transmittance obtained varied between 70 and 90% while energy gap varied between 2.45 and 2.48 eV.

Amanullah *et al.* (2005) doped (CdS) thin films with chlorine onto glass substrates by CBD and their structural analysis showed the films having both hexagonal and cubic phases. Electrical resistivity was in the range 10^6 - $10^8 \Omega \text{ cm}$ for CdS and low resistivity for CdS:Cl annealed films (10^{-2} - $10^2 \Omega \text{ cm}$) with n -type conductivity.

Nnabuchi *et al.* (2010) doped CdS with cobalt by chemical bath deposition. The transmittance was high (above 70%), the reflectance was low (below 20%) and moderate band energy gap (approximately 2.1 to 2.5 eV). Thus, CdCoS was found suitable for window layers for photocells.

Modafferet *et al.* (2009) prepared Pb_xCd_{1-x}S thin films using cadmium as a dopant in the composition range of $0.05 \leq x \leq 0.25$, using CBD and the films exhibited varying direct band gap from 1.3 eV to 2.4 eV with desirable window layer properties.

2.3.4 CdSe/Cu₂S and CdS/Cu₂S solar cells

Among all kinds of solar cells, cadmium sulphide (CdS) cells are the most widely researched but their efficiencies are limited by several factors (Altosaaret *al.*, 2004). Siu and Kwok (1978) made a study of the CdS/Cu_xS thin-film solar cells. The solar response investigated was found to depend on film thickness, grain-size, grain structure, spectral responses and I-V characteristics.

Ashour(2006)extended the work of Siu and Kwok (1978) and deposited CdS and Cu₂S thin films on a glass substrate, Cu₂S layer by the dry method and a CdS/Cu₂S hetero-junction by high vacuum evaporation (HVE). The fabricated cell had the efficiency of about 7.2%.

Bayhan (2006) fabricated solar cell (CdS:In/CdTe:Sb) on tin oxide(TO) coated glass substrates and annealed at 200⁰C in a nitrogen gas atmosphere.The practical efficiency obtained was 16.5%.

2.4 Improving optical and electrical properties of CdSeS/Cu₂S solar cells

Incident light of sufficient energy when incident on a *p-n* junction, it creates electron-hole pairs. If the energy of photons is sufficient then current flows (Al-Ayashi, 2007). Energy generated this way was first produced by a French scientist, A.E. Becquerel in 1839 (Nault, 2005) and in 1883 a functioning solar cell was built by Charles Fritts. In order to improve the optical and electrical properties of CdS thin films, doping has been done using various dopants and methods.

Reports on a solar cell with *n*-type Cd_xSe_{1-x}S and *p*-type Cu₂S are limited. Thin films of CdSeS can be chemically deposited using cadmium salt, thiourea and sodium seleno-sulphate. The optical absorption studies show that doping the CdS thin films increase the short circuit current and open circuit voltage in *p-n* junctions attributed to minimized window absorption losses (Al-

Ayashi, 2007). Doping of CdSe with sulphur is expected to increase energy gap, decrease window absorption losses and decrease the lattice mismatch of CdSeS as in the CuInGaSe semiconductors (Singh and Bhushan, 2008).

The challenge of using ternary semiconductors to replace binary and silicon semiconductors for solar cells has shown interest in recent researches. This study therefore aims at optimizing $\text{Cd}_x\text{Se}_{1-x}\text{S}$ thin film and also to fabricate a cheap solar cell using simple chemical bath deposition method (CBD).

CHAPTER 3

THEORY OF THIN FILMS AND P-N JUNCTION

3.1 Introduction

This chapter explains the theory of semiconductor thin films, their electrical and optical properties and their applications in solar cell fabrication. The chapter discusses the performance of solar cells and their limitations in energy conversion efficiency.

3.2 Semiconductor thin films

Semiconductor materials have electrical resistivity value falling between that of an insulator and a conductor. Thin films have thickness measurements ranging from nanometers to micrometers. Solar cells are basically made from thin films of p-n semiconductors that convert photons into electricity by a process called photovoltaic effect (Markvat, 1998). Thin film semiconductors are most researched materials for photovoltaic applications. Thin film semiconductor technology tends to lower costs and also lower material consumption (Shadia *et al.*, 2008).

3.3. The p-n Junction

The p-n junction has two-terminals with an n-doped and a p-doped region. Electrical devices like p-n diodes, light emitting diodes, photo-detectors and transistors are basically p-n junctions. The p-n junction is formed in a single crystal of semiconductor by making one terminal of the crystal p-type by doping it with acceptor atom and making the other terminal n-type by doping with donor atoms. The region where p-type and n-type meet is the junction (Robert *et al.*, 2008; Thomas, 2008)

The figure 3.1 represents a p-n junction. When p-type and n-type are in contact they form a junction. The majority carrier of each type diffuses across the junction. The majority carrier (holes) from p-type diffuses to n-type material and the majority carrier of n-type diffuses to p-type material.

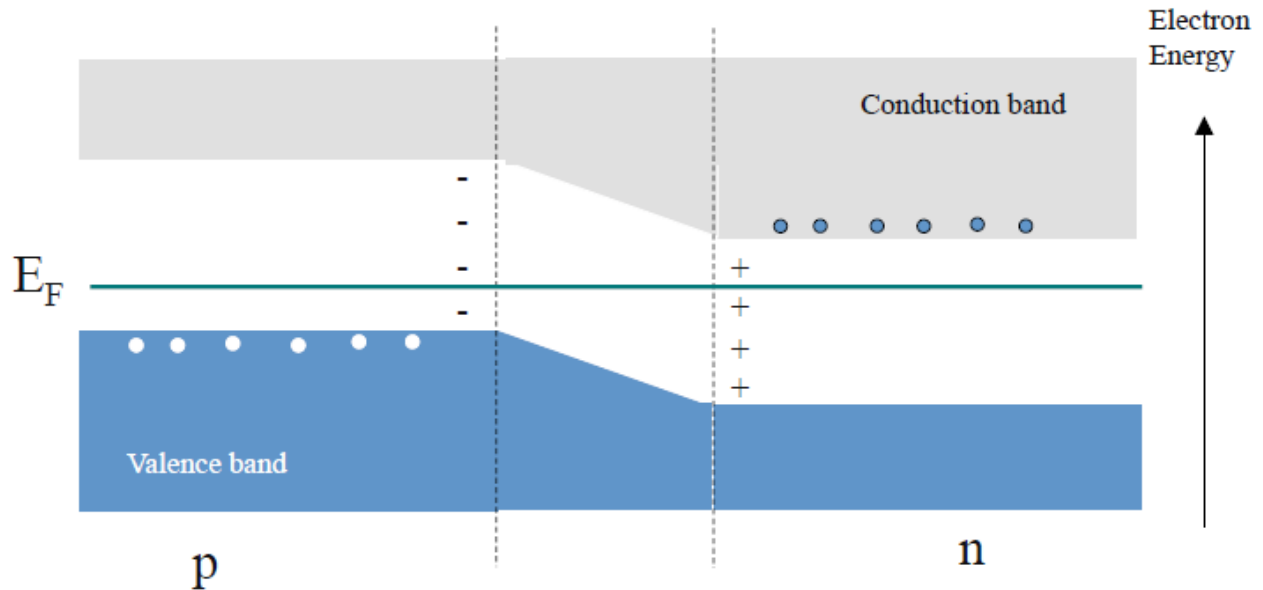


Fig. 3.1: A typical p-n junction(Dilli, 2008).

Diffusion of electron from n-type leaves a positive donor ion behind on the n- side. Likewise the hole diffuses from p-type to n-type. The free electrons and holes recombine. Recombination eliminates diffused electrons and holes. Consequently, only charged ions adjacent to the junction in a region without mobile carriers (called depletion region) is left. The net positive ions create an electric field that generates a force that opposes the continued exchange of charge carriers(Zeman, 2003). The electric field created drifts the minority carrier in the opposite direction across the junction. Thus when equilibrium attained, the drift carriers and diffused carriers should be balanced in magnitude and in opposite direction(Yilmaz, 2004). The figure 3.2 shows the influence of photon energy on a p-n junction. Conduction in *p-n* junction involves conduction band and valence band. Electrons flow in the conduction band, whereas the hole flows in the valence band. At equilibrium, the minority hole and electron drifts easily under the influence of built-in electric field E .

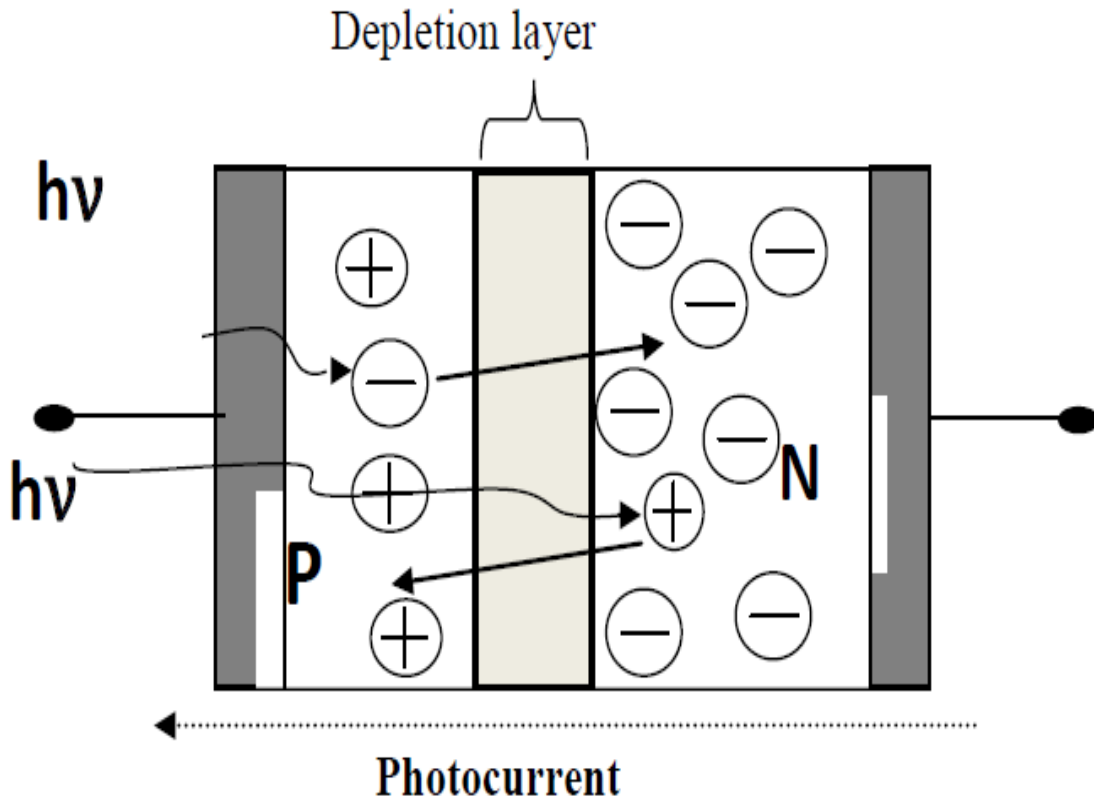


Fig. 3.2: Ap-n hetero-junction under illumination (Markvat, 1998).

The diffusion majority carriers have to overcome the potential barrier V_B of the junction created as the result of depletion region. This means that majority carrier should at least acquire energy of an electron volt before it can overcome the barrier and diffuse into either p or n region. Figure 3.3 shows band diagram showing the location of the carrier at equilibrium condition (Abdullah, 2007).

3.4 Photovoltaic effect and solar cells

Photovoltaic effect is a process by which a solar cell converts sunlight (electromagnetic radiation) into electrical energy. Quantum theory explains that electromagnetic radiation is quantized into photons. The energy of photon (E_{ph}) depends on the frequency of the light as shown by equation 3.1 (Johansen, 2004):

$$E_{ph} = hf = \frac{hc}{\lambda} \quad (3.1)$$

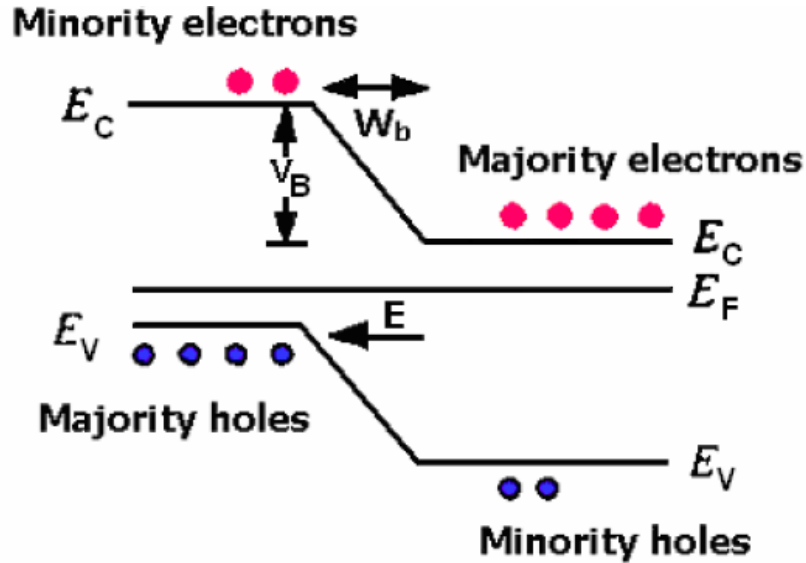


Fig. 3.3: The energy band diagram of a *p-n* junction (Floyd, 2012)

where f is the frequency and λ is the wavelength of the radiation, h is Planck's constant and c the speed of light. The photon energy must be higher than the energy band gap of a semiconductor to excite the electrons from the Valence band to conduction band. Consequently, the higher energy electrons move from the solar cell into the external circuit.

3.5 Energy band gaps in semiconductors

Omar(1975) defines the energy gap (E_g) as the energy difference between the maximum valence band (E_V) and the minimum conduction band (E_C) as illustrated in figure 3.4.

Insulators do not have free electrons so as to conduct current electricity because all the electrons form strong bonds between neighbouring atoms. However, semiconductors have rather weaker covalent bonds that can break by heat. When these bonds break, electrons travel from the valence

band to the conduction band thus leaving electron charge deficiency in the valence band(Jain *et al.*, 2006).

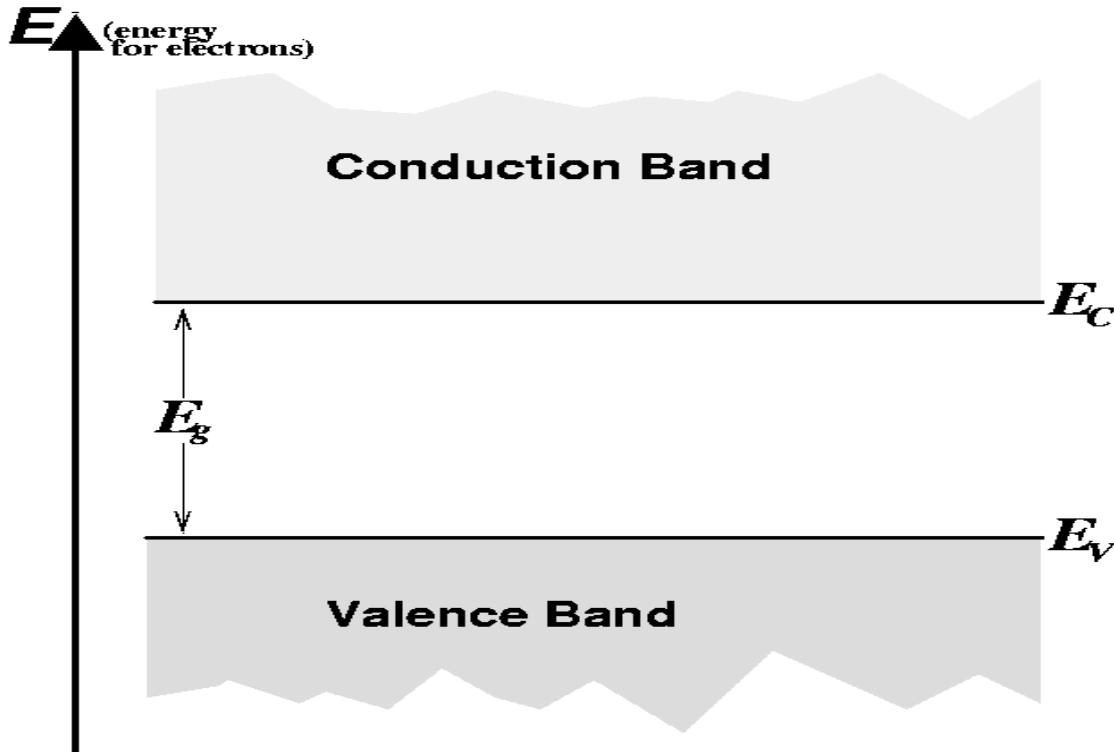


Fig. 3.4: Conduction band, valence band and energy band gap (Dilli, 2008)

Semiconductors have a negative temperature coefficient of resistivity. The resistivity decreases as they absorb more heat. Therefore, as the temperature of the semiconductor increases thus its conductivity. At room temperature (300K) and under normal atmospheric pressure silicon and gallium arsenide have band gaps 1.12eV and 1.42eV respectively.

According to Schroder(1998)inconductors the conduction band is either partly filled or overlaps the valence band. In other words there is no band-gap. As a consequence, current conduction can readily occur in conductors.

3.6 Intrinsic carrier concentration and fermi energies

Intrinsic charge carriers affect the conductivity of semiconductor materials. The electron density n is a product of the $N(E)$ and the $F(E)$. Hence, the conduction band electron density (n) is given by integration as shown by equation 3.2 (Zeman, 2003):

$$n = \int_{E_c}^{E_{top}} N(E)F(E)dE \quad (3.2)$$

where $N(E)$ is the density of allowed energy states per unit volume and $F(E)$ probability of occupying that energy. Equation 3.3 shows that the density of allowed energy is (Zeman, 2003):

$$N(E) = 4\pi \left(\frac{2m_n}{h^2} \right)^{3/2} E^{1/2} \quad (3.3)$$

where h is Planck's constant. $F(E)$ is given by the Fermi-Dirac distribution function below (equation 3.4):

$$F(E) = \frac{1}{1 + e^{(E-E_F)/kT}} \quad (3.4)$$

where k is the Boltzmann constant, T is the absolute temperature, and E_F is the Fermi energy level. If we let $(E-E_F) \gg 3kT$, in expression 3.4 the density of the electron in the conduction band can be shown by equation 3.5 to as (Zeman, 2003):

$$n = N_C e^{-\frac{E_c - E_F}{kT}} \quad (3.5)$$

$$\text{where } N_C \equiv 2 \left(\frac{2\pi m_n kT}{h^2} \right)^{3/2}$$

where N_C is the effective density of states in the conduction band, m_n is the effective mass of the electron. In a similar manner, the hole density p in the valence band may be obtained by equation

3.6 as:

$$\eta = N_v e^{-\frac{E_c - E_F}{kT}} \quad (3.6)$$

$$\text{where } N_v \equiv 2 \left(\frac{2\pi m_p kT}{h^2} \right)^{3/2}$$

where N_v is the effective density of states in the valence band and m_p is the hole effective mass.

In a pure semiconductor the number of electrons (n) and holes (p) are equal in conduction and valence bands respectively. That satisfies the expression ($n = p = n_i$) where n_i is the intrinsic carrier density. The Fermi level for an intrinsic semiconductor by equation 3.7 is obtained by equating equations 3.5 and 3.6:

$$E_F = E_i = \frac{E_c + E_v}{2} + \frac{3kT}{4} \ln \left(\frac{m_p}{m_n} \right) \quad (3.7)$$

At 25°C, the intrinsic Fermi level E_i of a semiconductor normally lies very close to the middle of the band-gap. The intrinsic carrier density n_i is also obtained directly from the equations 3.5 and 3.6

$$np = n_i^2 \quad (3.8)$$

$$n_i^2 = N_C N_V e^{\left(\frac{E_V - E_C}{kT} \right)} \quad (3.9)$$

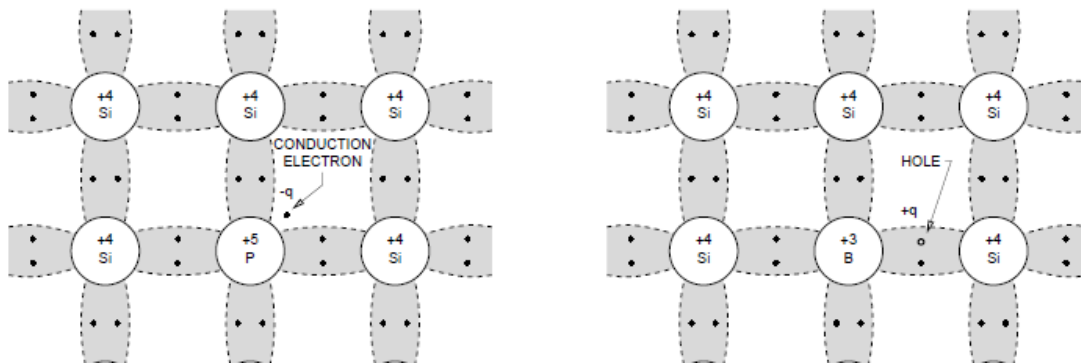
$$n_i = \sqrt{N_C N_V} e^{\left(-\frac{E_g}{2kT} \right)} \quad (3.10)$$

The relation in equation (3.8) is the mass action law. The relation is applicable for both intrinsic and extrinsic semiconductors under a thermal equilibrium condition.

3.7 Doping of semiconductors

Intrinsic semiconductors are un-doped semiconductors such as silicon and germanium. When impurities are added to pure semiconductors they become extrinsic semiconductors. Process of

adding impurities is known as doping. Doping alters the lattice structure of pure semiconductors. Impurities like phosphorus makes the semiconductor n-type material because of the net negative charge carrier as shown in diagram 3.5a. Doping Si with boron creates an electron deficiency thus the p-type semiconductor is formed as shown by the figure 3.5b.



3.5 (a)

3.5 (b)

Fig 3.5 Effect of doping Silicon with (a) phosphorus and (b) boron (Johansen, 2004)

Fig. 3.5 is schematic diagram of energies of doped lattices. A donor is ionized by accepting a valence electron.

3.8 Current conduction in semiconductors

3.8.1 Intrinsic charge carriers

When covalent bonds are broken free electrons move about in the crystal, or recombine with positive germanium ions. At thermal equilibrium the recombination rate and the ionization rates are equal. The current moves through the periodic potential of the silicon lattice quite the opposite of the positive charges that are rigid within the atomic nuclei of the lattice.

3.8.2 Extrinsic charge carriers

The intrinsic conductivity of Si is increased by doping. Elements used in semiconductor doping rather introduce energy levels into the band-gap. A shallow donor will have an energy level N_D in

the band gap nearer the lowest conduction band energy E_C , and a low acceptors state E_A is in the same way located in the band-gap close to the highest valence band energy E_V . Phosphor and boron are both shallow dopants in silicon as they introduce a shallow acceptor state in silicon. When all the donor or acceptor impurities are ionized at room temperature, an equal number of electrons and holes in the conduction band and valence band formed respectively. Equation 3.11 and 3.12 describes the complete ionization as:

$$n = N_D \quad (3.11)$$

$$p = N_A \quad (3.12)$$

where N_D is the donor concentration, n is the electron density, p is the hole density and N_A is the acceptor concentration. In case of complete ionization of an n-doped material at 25°C , the Fermi level is calculated by equation 3.13 as: (Dilli, 2008)

$$E_C - E_F = kT \ln \left(\frac{N_C}{N_{CD}} \right) \quad (3.13)$$

in the same way a p-doped material it is easily revealed by equation 3.14 as:

$$E_F - E_V = kT \ln \left(\frac{N_V}{N_A} \right) \quad (3.14)$$

It is observed that for high donor concentrations, the variation $(E_C - E_F)$ is reduced, that's why the fermi level will move nearer to the bottom of the conduction band. Similarly, a high acceptor concentration will move the fermi level closer to the valence band (Omar, 1975; Abdullah, 2007). It implies that for extrinsic semiconductors, the fermi level is diverse from the intrinsic fermi level.

3.8.3 Drift current (Mobility)

The electrons in motion possess kinetic energy given by equation 3.15 (Johansen, 2004):

$$\frac{1}{2} m_n v^2 = \frac{3}{2} kT \quad (3.15)$$

where m_n is the effective electron mass, v is the average thermal velocity, k is the Boltzmann's constant and T is the absolute temperature. At room temperature the thermal velocity in equation 3.16 (b) is about 10^7 cm/s for Si and GaAs. The drudemodel Theiss (2002) assumes that the conduction electrons move about freely in a static lattice of positive ions forming a gas of conduction electrons verified using the kinetic theory method. Once an electric field is applied, each electron is accelerated in the field direction thereafter its velocity is normalized over again. The momentum applied to an electron is $-q\varepsilon\tau_c$, and the momentum gained is $m_n v_n$ where v_n is called the drift velocity. We have: (Johansen, 2004);

$$-q\varepsilon\tau_c = m_n v_n \quad (3.16 \text{ (a)})$$

$$v_n = - \left(\frac{q\tau_c}{m_n} \right) \varepsilon \quad (3.16 \text{ (b)})$$

which describes the proportionality factor (electron mobility/ cm^2/Vs) of the drift velocity to the electric field applied as: (Johansen, 2004).

$$\mu_n \equiv \frac{q\tau_c}{m_n} \rightarrow v_n = - \mu_n \varepsilon \quad (3.17)$$

Analogous expression may be written for holes in the valence

$$v_p = \mu_p \varepsilon \quad (3.18)$$

Equation 3.18 describes the relationship between the mobility and the mean free time both of which depends on various scattering processes. The two important scattering mechanisms are lattice scattering and impurity scattering. Lattice scattering results from thermal vibrations of the lattice atoms caused by the temperature rise above 273K.

3.8.4 Influence of applied electric field on charge carriers

The drift current produced as a result of charge carriers are transported under influence of an applied electric field. At the same time, free electrons in a semiconductor will experience a force $q\varepsilon$ equal to the negative gradient of the potential energy (E) shown by equation 3.19 as:

$$-q\varepsilon = -\frac{dE_c}{dx} \rightarrow \varepsilon = \frac{1}{q} \frac{dE_c}{dx} = \frac{1}{q} \frac{dE_i}{dx} \quad (3.19)$$

For a homogeneous material, ε is constant all over the sample. The accelerated electron in the field gains kinetic energy as it loses potential energy. A sample with a cross-sectional area A, placed in a homogeneous electric field, its electron current density J_n possibly will be found by expression 3.20 as (Zeman, 2003):

$$J_n = \frac{I_n}{A} = \sum_{i=1}^n (-qv_i) = -q_n v_n = q_n \mu_n \varepsilon \quad (3.20)$$

J_n represents the electron current. A similar argument applies to holes yielding $J_p = q_p \mu_p \varepsilon$, so the total current density as a result of the applied field may well be written as by equation 3.21:

$$J_n = J_n + J_p = (q_n \mu_n + q_p \mu_p) \varepsilon = \sigma \varepsilon \quad (3.21)$$

The conductivity σ , equivalent of reciprocal of resistivity is:

$$\rho \equiv \frac{1}{\sigma} = \frac{1}{q(n\mu_n + p\mu_p)} \quad (3.22)$$

Normally, in extrinsic semiconductors, one of the current components is major because of the great difference between the two carrier densities. Thus, equation (3.22) is reduced to:

$$p \approx \frac{1}{q_n \mu_n} \text{ for an n-type semiconductor} \quad (3.23)$$

$$\rho \approx \frac{1}{q_p \mu_p} \text{ for a p-type semiconductor} \quad (3.24)$$

3.8.5 Diffusion current

In semiconductors diffusion currents occur at locations with a non-uniform charge distribution. In consequence, the charge carriers move away from a high concentration of charge carriers of the same sign to the direction of lower concentration. Equally diffusion currents of carriers of the opposite polarity shift in the opposite direction. Drift currents exist also in regions with a non-zero spatial charge distribution gradient as a result of the electric field produced by the non-uniformity. The current J_n is a consequence of the flow of electrons as shown by equation 3.25 (Zeman, 2003).

$$J_n = -qF = qD_n \frac{d_n}{dx} \quad (3.25)$$

Where, F denotes the rate of current flow, D_n diffusivity and q the electric charge. It is observed that both the electron concentration and current increase in the same positive direction (x-direction), accordingly the electrons flow in the opposite direction. The total diffusion and drift current for both the electrons and holes gives the total conduction current density. Diffusion currents and Drift are components that superimpose on each other. Diffusion may be explained by one dimensional first order approximation.

3.9 Types of band gaps

Mainly there are two types of band gaps in semiconductors: Direct and indirect semiconductor.

3.9.1 Direct band gap semiconductors

Those materials for which maximum of valence band and minimum of conduction band lie on same value of k , called direct band-gap materials as in figure 3.6i.e. satisfies the condition of energy and momentum conservation. For example: GaAs, InP, and CdS.

Absorption Spectroscopy is used to determine whether a band gap is direct or indirect by plotting $(\alpha h\nu)^2$ versus photon energy ($h\nu$). The value of the band gap is obtained by the Tauc relation. Tauc (1974) shows derived relation in equation 3.26 (Vajpeyi, 2011).

$$(\alpha h\nu) \approx A(\sqrt{h\nu - E_g}) \quad (3.26)$$

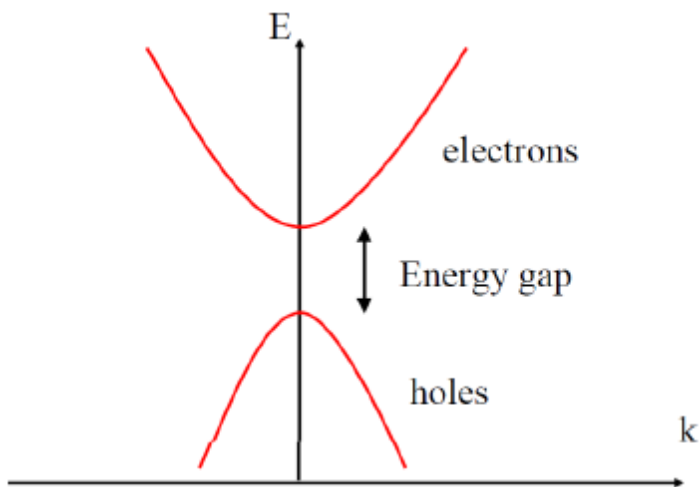


Fig. 3.6 E-k diagram of a direct band gap semiconductor (Vajpeyi, 2011)

If a linear part of a plot of $(\alpha h\nu)^2$ versus $(h\nu)$ is extrapolated then there is a direct band gap, measurable on the x-axis of a graph where the $\alpha = 0$ axis

3.9.2 Indirect band gap semiconductors

Those materials for which maximum of valence band and minimum of conduction band do not occur at same value of k vector, called indirect band-gap materials as in figure 3.7 for example: Si and Ge.

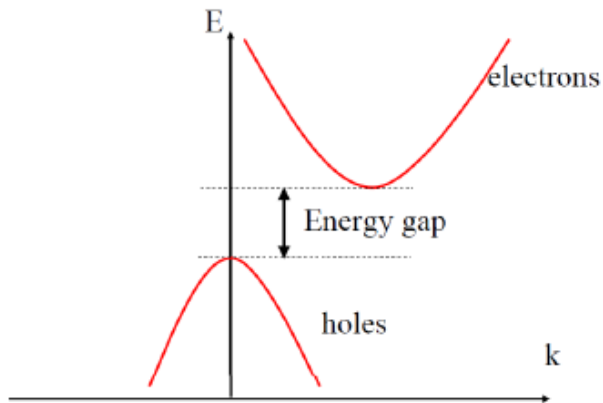


Fig. 3.7 E-k diagram of indirect band gap semiconductors (Vajpeyi, 2011)

In view of the fact that the E_g transition of an electron in an indirect semiconductor require a non-zero crystal momentum change. Consequently, direct generation or recombination is not likely to take place. To a certain extent an indirect process is more likely wherever electrons step through localized intermediary energy states in the forbidden band-gap. These transitional states are called recombination centers. The captured electrons by recombination centers may either be transferred to the conduction or to the valence band.

3.10 Thin film applications

Thin films have a variety of applications. Magnetic thin films are useful in making sensors and solar cells. Thin films technology is usefully employed in Smart windows and information storage. In optics, laser mirrors and transmission enhancing coatings are manufactured. In electronics, integrated circuits are made of layers of insulators, semiconductors and conductors (Choi *et al.*, 2003; Lawrence *et al.*, 2008; Robert, 2008).

3.11 Performance of a solar cell

The thicker p-type layer absorbs most of the incident light that generates an electron-hole pair. The holes and electrons are then separated by the solar cell. The electrons diffuse to the junction and thus generating electrical power. The electrical power is collected by both back and front metal contacts.

3.11.1 Light trapping

Light trapping through the thick layer is enhanced using sophisticated arrangements (Brendel and Queisser, 1993). In crystalline Silicon solar cells, open circuit voltage is increased by light trapping and reducing the thickness of the cell (Markvart, 2000). Reflection from the window layer can be reduced by the use of an anti-reflecting coat (ARC) and adding texture on bare silicon. The figure 3.8 shows experimental results of effects of adding ARC and texture on the bare silicon (Born and Wolf, 1999).

Goetzberger *et al.* (1998) found that reflection coefficients reduced by using anti reflection coating (ARC) on bare silicon. The reflection coefficient was further lowered by texturing the surface of the single layer ARC. Therefore, applying an ARC and texturing enhances light trapping on the solar cell surfaces.

3.11.2 Solar cell parameters

A solar cell in the dark is a semiconductor current rectifier, or diode (Sze, 1981). The photo generated current depends on the wavelength of light and the photon flux incident on the cell (Philips *et al.*, 1997). In terms of the quantum efficiency or spectral response the photo-generated current is usually independent of the applied voltage (Hegedus, 1997; Hishikawa *et al.*, 2000) as shown by equation 3.27 below:

$$V_{oc} = \frac{k_B T}{q} \ln \left(1 + \frac{I_{ph}}{I_0} \right) \quad (3.27)$$

where K_B is the Boltzmann constant, T is the absolute temperature, q is the electron charge, and V is the voltage at the terminals of the cell and I_0 is the diode saturation current (Sze, 1981).

The I-V characteristics of a solar cell are explained by figure 3.9. The maximum voltage the solar cell can develop is V_{oc} while the short circuit current of the solar cell is I_{sc} . If the cell could simultaneously deliver maximum current and the maximum voltage, the maximum power (P_m) would be $P_m = V_{oc} \times I_{sc}$. However, the actual power is given by $P_m = V_m \times I_m$. (Al-ayashi, 2007).

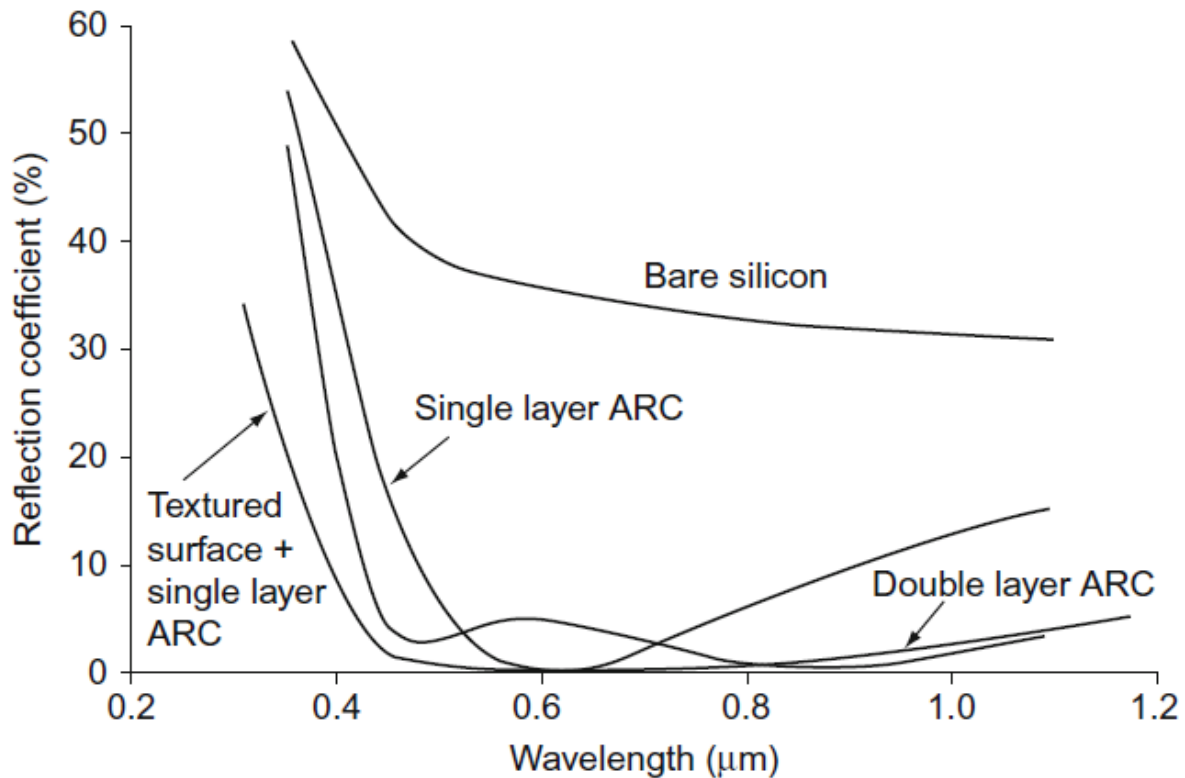


Figure 3.8 Comparison of the reflection coefficient of different silicon layers (Zweibel and Hersch, 1984 ; Goetzberger *et al.*, 1998).

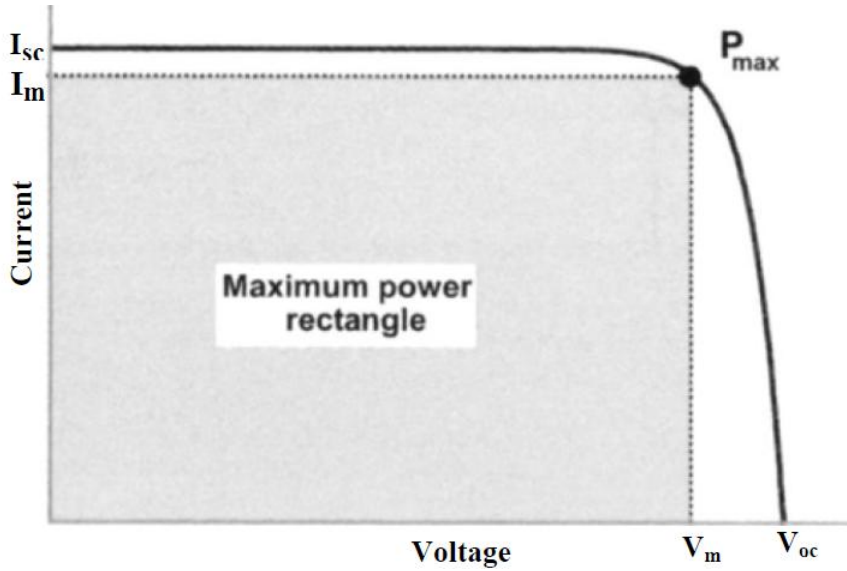


Fig. 3.9 The typical I-V characteristics of the solar cell (Al-ayashi, 2007)

The solar cell fill factor (FF) is thus defined as (Udaet *al.*, 1990):

$$FF = \frac{I_m V_m}{I_{sc} V_{oc}} = \frac{P_{max}}{I_{sc} V_{oc}} \quad (3.28)$$

3.11.3 Solar cell conversion efficiency

The conversion efficiency of solar cells is the ratio between the generated maximum power, P_m , generated by a solar cell and the incident power P_{in} . The incident power is equal to the irradiance of AM1.5 spectrum, normalized to 1000 W/m^2 (Al-Ayashi, 2007). The efficiency, η is determined from the I - V measurement using Equation. 3.29 (Al ayashi):

$$\eta = \frac{P_m}{P_{in}} = \frac{P_{mp} V_{mp}}{P_{in}} = \frac{I_{sc} V_{oc} FF}{P_{in}} \quad (3.29)$$

Where V_{oc} is the open circuit voltage, I_{sc} is the short circuit current, FF is fill factor, P_m is maximum power output and P_{in} is the power incident on the solar cell.

3.12 Conversion efficiency limits

3.12.1 Spectral mismatch

Photons carrying less energy than the material band gap are not absorbed because they do not have enough energy to generate electron-hole pair (Marko and Marko, 2014). The photons with energy greater than the thin film band gap are absorbed in the p-type layer of a solar cell. However, excessive energy is released as heat into the semiconductor lattice (Henry, 1980). Therefore, according to Marko and Marko (2014) spectral losses can be caused by unabsorption of photons with energy below band gap as well as thermalization of absorbed photons. Spectral mismatch contribute to over 50% drop of the conversion efficiency of a solar cell.

3.12.2 Reflectance

Refractive index (n) and extinction coefficient (k) are optical constants expressed by a complex function, $\tilde{n} = n - ik$. Incident light on junction is wavelength dependent transmittance $T(\lambda)$ and reflectance, $R(\lambda)$. Reflectance is the ratio of the energy bouncing off at the surface of the interface to the total incident energy. Multiple reflectance between the air and among layers of thin films result in loss of usable and useful light energy.

3.12.3 Shading losses

Most solar cells have metal contacts on the front side of the cell which decreases effectively the active area of the solar cell. The size of the front contact should be designed to minimize photon energy losses besides the losses due to the series resistance of the contact (Al-Ayashi, 2007).

3.12.4 Absorption loss

When light penetrates into the active layer of a solar cell, not all the light is absorbed. Incomplete absorption due to limited thickness of the layer or low refractive index contributes to the low efficiency of solar cells (Al-Ayashi, 2007).

3.12.5 Collection losses

Minority of charge carriers recombine after generation at the surfaces of the junction (Green, 2002). Therefore recombination lowers the efficiency of the solar cell.

3.12.6 Recombination and series resistance

Doping of semiconductor materials determines the quality of the p-n junction formed. The quality also influences the open circuit voltage of the junction which is basically a solar cell. The desirable quality material of a junction should minimize recombination and also minimize series resistance of metal contacts (Abdullah, 2007).

Recombination of charge carriers in the junction and series resistance of a solar cell decreases the fill factor FF from 100% to a lower value. Given that FF is a function of V_{oc} practical values of V_{oc} and by extension efficiency falls.

CHAPTER 4

EXPERIMENTAL PROCEDURES

4.1 Introduction

This chapter broadly discusses the chemical bath deposition experimental procedures for thin films deposition, cleaning of substrates, deposition and characterization of Cu_2S and CdSeS thin films by chemical bath deposition technique. The chapter ends with the fabrication and characterization of the solar cell.

4.2 Materials for thin film deposition

4.2.1 Deposition of p-type Cu_2S thin films

The copper (I)sulphide thin films requirecopper II sulphate (CuSO_4) as a source of copper (II) ions and 0.1M thiourea $\{\text{CS}(\text{NH}_2)_2\}$ as a source of sulphide (S^{2-}) ions . The concentration of the Copper (II)sulphatewas varied from 0.1M to 0.5M in the reaction bath. Tartaric acid ($\text{H}_6\text{C}_4\text{O}_6$) was used a complexing agent. De-ionized water was usedto dissolve the solid compounds to form a homogenous reaction bath. The Hydrochloric acid was used to lower the pH of the precursor solution.

4.2.2 Deposition of CdSeS

Deposition of cadmium selenosulphiderequires the source of cadmium from cadmiumnitrate $\text{Cd}(\text{NO}_3)_2$. Thiourea $\{\text{CS}(\text{NH}_2)_2\}$ was selected as a source of sulphide (S^{2-}) ions. Sodium selenosulphatewas used as a source of selenium ions. Ammonium nitrate was used to control the pH of the precursor solution.

4.3 Cleaning of the glass substrates

Glass microscope slides were cleaned by degreasing them in concentrated nitric acid (HNO_3) for 20 minutes. The slides were soaked in hot acid to create nucleation centers and washed in detergent solution, rinsed in distilled water and dried in air at room temperature.

4.4 Experimental set-up

Figure 4.1 is a set up comprising the retort stand to hold a thermometer and the glass substrate. The magnetic stirrer rotates to ensure that most of the reactants are well mixed to facilitate formation of uniform thin film onto glass substrate. The rotor or magnetic stirrer can be used interchangeably. The glass substrate is suspended into the precursor solution. The heater raises the temperature of the precursor so as to maintain fairly constant temperature measured by the thermometer.

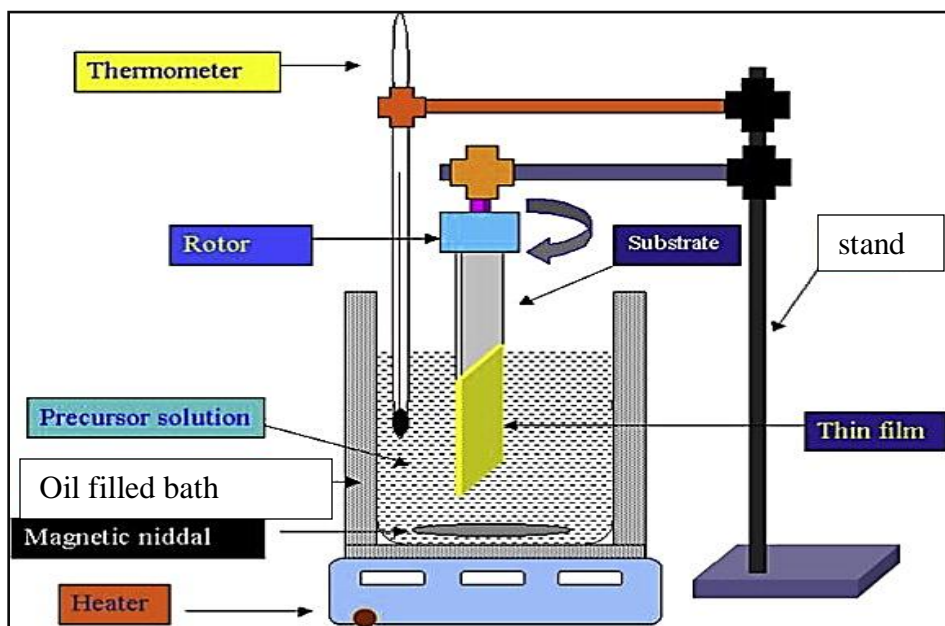


Figure 4.1: Chemical bath deposition set up used in this research.

4.5 Procedure

4.5.1 Deposition of Cadmium Seleno-sulphate thin films

Details of bath constituents for preparation of $Cd_xSe_{1-x}S$ are shown in the Table 4.1.

Table 4.1 Composition of Bath constituents for preparing $Cd_xSe_{1-x}S$

Molarity of 20(ml) $Cd(NO_3)_2$ (x) ± 0.05	Molarity of thiourea 20(ml) $CS(NH_2)_2$ ± 0.05	0.008M NH_4NO_3 Volume (ml) ± 0.5	Molarity of Na_2SeSO_4 20 (ml) (1-x) ± 0.05
1.0	0.5	2	0.0
0.8	0.5	2	0.2
0.6	0.5	2	0.4
0.4	0.5	2	0.6
0.2	0.5	2	0.8

Molar concentrations of the reagents were prepared in distilled water and were put into 5 separate beakers. All the reagents were poured into 100ml glass beakers while stirring. The mixture in 100ml beaker was put into about $60^{\circ}C \pm 2$ water bath. While stirring the mixture, about 29.4% of Ammonia solution (NH_4OH) was added drop wise to maintain the pH of the solution to a value of 9.

When the temperature of the mixture was about $60^{\circ}C$, clean substrates were mounted vertically in the bath beaker for about 30 minutes. After deposition time (30minutes), the coated glass slides were rinsed with distilled water and dried in air at room temperature. Doping to obtain

$Cd_xSe_{1-x}S$ was done by varying the molarities of reagents used as in Table 4.1. The value of x varies from 1.0 to 0.2 according to the chemical formula $Cd_xSe_{1-x}S$.

4.5.2 Deposition of copper (I) sulphide Cu_2S thin films

To deposit Cu_2S , analytical grade prepared copper (II) sulphate $CuSO_4$, hydrochloric acid (HCl), Thiourea ($CS(NH_2)_2$) and tartaric acid in de-ionized water was mixed as shown in the details of the bath constituents shown in the Table 4.2 below.

Table 4.2 Composition of reagents used to deposit copper (I) Sulphide (Cu_2S) thin films

copper (II) sulphate $CuSO_4$		0.2M thiourea volume (ml)	0.2M tartaric acid Volume(ml)	PH	Time(min)
Concentration ± 0.05	Volume (ml) ± 0.5	$CS(NH_2)_2$ ± 0.5	$H_6C_4O_6$ ± 0.01	-	-
0.1M	25	25	25	3	20
0.2M	25	25	25	3	20
0.3M	25	25	25	3	20
0.4M	25	25	25	3	20
0.5M	25	25	25	3	20

The bath constituents were heated to a temperature of $40^\circ C \pm 2$. Using pH meter its pH was maintained at 3 by adding dilute HCl drop wise while stirring for 20 minutes. Glass substrate was dipped vertically into the deposition bath for about ten minutes. The glass substrate was detached from the beaker and washed in de-ionized water to remove the loosely adhered powder precipitates in the solution during deposition and then dried in air at room temperature. Concentration of $CuSO_4$ was varied from 0.1M to 0.6M at intervals of 0.1M.

4.6 Characterization of thin films procedures

4.6.1 Optical characterization of thin films.

UV-VIS NIR 3700 Spectrophotometer was used to measure transmittance and reflectance. Optical constants like absorption coefficient (α), extinction coefficient (k) refractive index (n), and band gap (E_g) were obtained by simulating transmittance. The schematic diagram of the analyzer is as shown in figure 4.2.

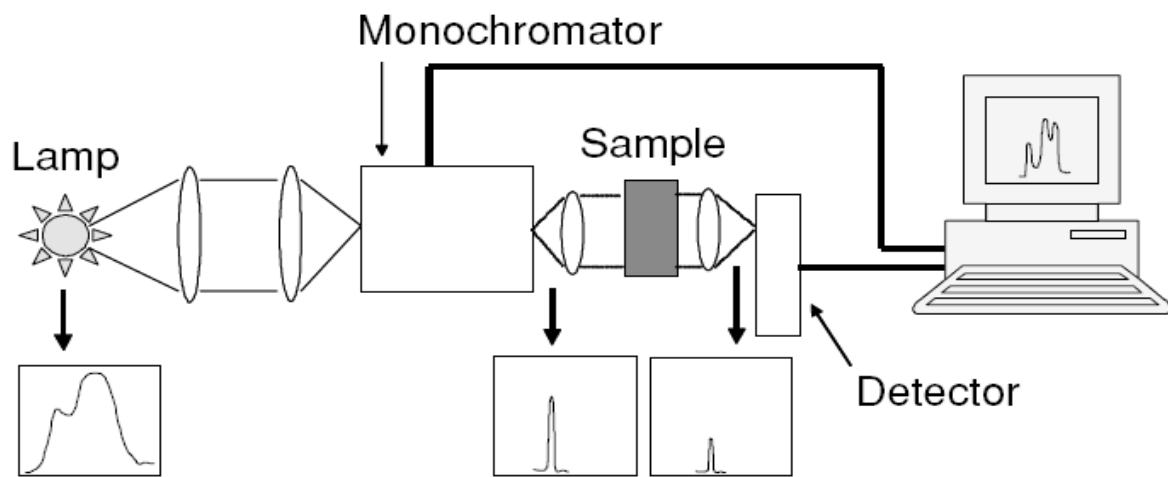


Fig 4.2: A schematic diagram of the spectrum analyser (Mosiori, 2012)

4.6.1.1 Refraction index and extinction coefficient

Optical properties are obtained from how light interacts with thin films. Light is an electromagnetic radiation that is affected by presence of charge along the path of propagation. These results in the change of wave velocity and intensity of radiation described by means of the complex index of refraction shown in equation 4.1.

$$N = n - ik \quad (4.1)$$

where n = real index of refraction, k = extinction coefficient, N = index of refraction of the film. So, after a film has been deposited, photons of wavelength, λ , and beam intensity, I_0 , are

usually directed at a film of thickness (l) and their relative transmission observed. Intensity of photons transmitted (I_t) through the film of thickness l is given by equation 4.2 (Zeman, 2003):

$$I_t = I_o e^{-\alpha l} \quad (4.2)$$

where I_o is virtual beam intensity of the photon, α is the absorption coefficient. Rearranging equation 4.2 above gives the expression for α as in equation 4.3;

$$\alpha = \frac{1}{l} \ln \left(\frac{I_o}{I_t} \right) (\text{cm}^{-1}) \quad (4.3)$$

where, I_R and I_o are intensities of the reflected and incident beams respectively.

4.6.1.2 The absorption coefficient and di-electric constant

The absorption co-efficient (α) and the dielectric constant (ϵ) relate as (UgwuandOnah, 2007) as equations 4.4 and 4.5:

$$\epsilon_r = n^2 - k^2 \quad (4.4)$$

$$\epsilon_i = 2nk \quad (4.5)$$

where (ϵ_r) is the real part and (ϵ_i) are the real and imaginary parts of the dielectric constants respectively. Refractive index (n) and extinction coefficient (k) of the material are explained by equation 4.6 (Abdullah, 2007):

$$k = \frac{\alpha \lambda}{4\pi} \quad (4.6)$$

where, (α) is the absorption co-efficient and wavelength of the radiation expressed by (λ). The optical conductance (σ_0) is obtained using the equation 4.7 below; (Abdullah, 2007),

$$\sigma_0 = \alpha n c \epsilon_0 \quad (4.7)$$

where (σ_0) is the optical conductance and (c) is the velocity of the radiation in the space.

4.6.1.3 The optical energy gap

The energy gap of the thin film is obtained by plotting $(\alpha h\nu)^2$ versus photon energy $(h\nu)$ (Ugwu and Onah, 2007). The straight-line part of the graph is extrapolated to meet the wavelength axis at λ_p at the point where $\alpha^2=0$. The band-gap is then obtained from the relation 4.8 below: (Ugwu and Onah, 2007);

$$E_g = \frac{hc}{\lambda_p} \quad (4.8)$$

4.7.2: Electrical properties

Resistivity and conductivity are the main electrical properties that characterize semiconductor thin films. The sheet resistivity of the thin films was measured by the four point probe method.

The measurements are made through four contact terminals on the thin film using Keithley 2400 Source meter. For sample thickness $t \gg s$ the probe spacing s , the integration between the middle probes where the voltage is measured gives equation 4.9 below: Amanullah, 2005);

$$R = \int_{x_1}^{x_2} \frac{\rho}{2\pi s} dx = \frac{\rho}{2\pi} \left[\frac{-1}{x} \right]_{x_1}^{x_2} = \frac{1}{2s} \left(\frac{\rho}{2\pi} \right) = \frac{\rho}{4\pi s} \quad (4.9)$$

where probe spacing (s) , is uniform. For $R = V/2I$, the sheet resistivity for a thin sheet becomes as equation 4.10 below:

$$\rho = \frac{\pi t R}{\ln 2} = \frac{\pi t V}{\ln 2 I} \quad (4.10)$$

Resistivity of the films was obtained using four point probe interfaced with Keithley 2400 source meter and computer. The results were presented in Tables and graphs.

4.8 Fabrication of the $\text{Cd}_x\text{Se}_{1-x}\text{S}/\text{Cu}_2\text{S}$ solar cell

A p-n junction $\text{Cu}_2\text{S}/\text{Cd}_x\text{Se}_{1-x}\text{S}$ was fabricated using the obtained optimum conditions like the concentration of the reagents, solution pH and temperature. After the deposition of the single clean layer thin film of $\text{Cd}_x\text{Se}_{1-x}\text{S}$, the Cu_2S was deposited by dipping the n-layer into the solution containing copper (II) sulphate, thiourea and tartaric acid at a temperature of 40°C for about twenty minutes and removed slowly. A silver paste was used as a front and back contacts. One side of the slide was wiped with cotton soaked in concentrated hydrochloric acid so as to keep the thin film deposited on one side only as shown in the figure 4.3.

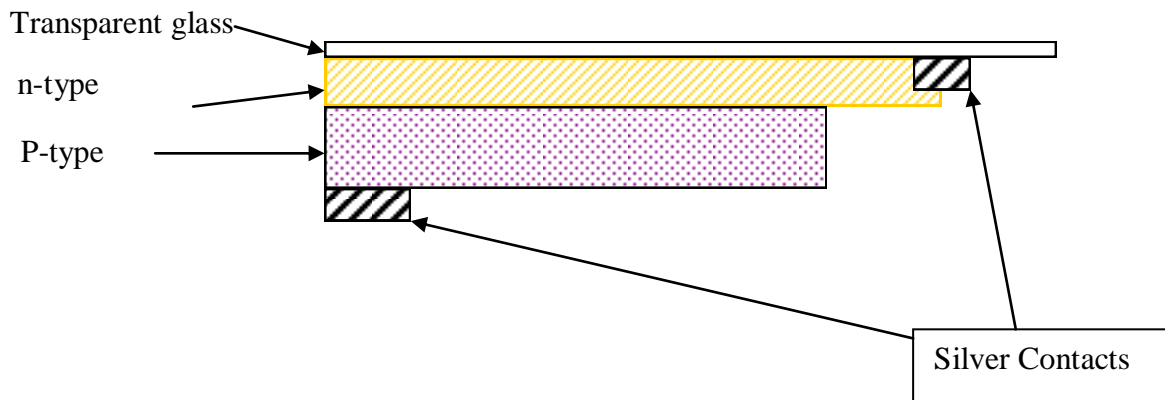


Fig. 4.3 Schematic cross- section of a solar cell

4.9 Characterization of solar cell

The I-V measurements of a solar cell were obtained by solar simulator connected in a system comprising the Keithley source-meter connected to computer system running labview programme. The measured data was used in plotting the I-V and power curves. From the curves, the short circuit current (I_{sc}), the open circuit voltage (V_{oc}), maximum current (I_{max}), maximum voltage and maximum output/ power was used in the relation 4.11 (Udahet *al.*, 1990):

$$FF = \frac{P_{max}}{V_{oc} I_{sc}} \quad (4.11)$$

Consequently, the value of solar cell conversion efficiency (η) was determined by relation 4.12 as:

$$\eta = \frac{I_{sc} V_{oc} FF}{E_{IRRAD} A_c} \quad (4.12)$$

where symbols retain their usual meanings as explained above.

CHAPTER 5

RESULTS AND DISCUSSION

5.1 Introduction

This chapter starts by presentation of the results obtained from investigated optical and electrical properties of both p-type (Cu_2S) and n-type (CdSeS) deposited thin films. The results are reported in Tables, figures and graphs. The chapter also reports on the I-V characteristics of the solar cell fabricated. Lastly, the values of measured characteristics are compared with the values of other researchers.

5.2 Optical properties of p-type Cu_2S

5.2.1 Transmittance

Figure 5.1 shows the optical transmittance spectra of Cu_2S thin films of different concentrations measured as a function of wavelength in the range of 300 nm to 1200 nm of incident photons.

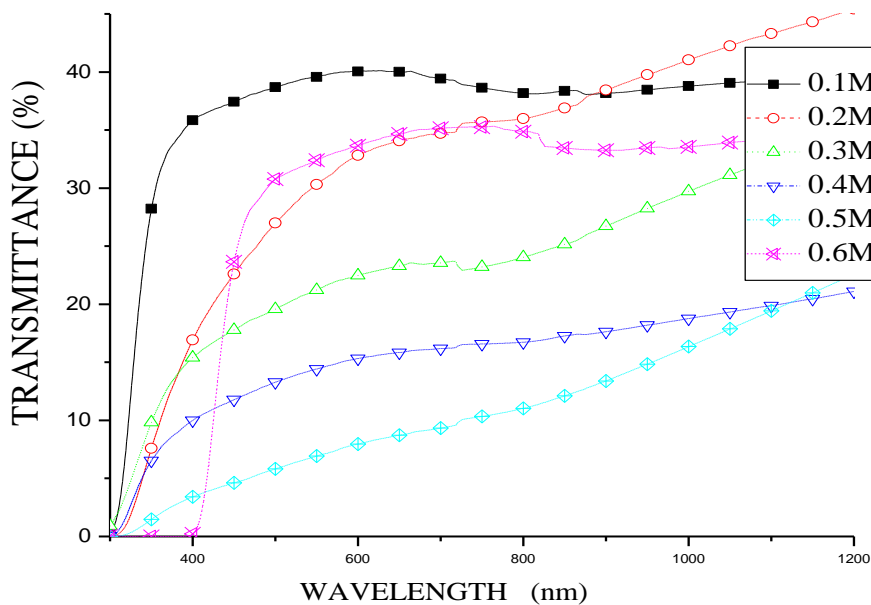


Fig. 5.1 Transmittance (T) as a function of wavelength (λ) for Cu_2S thin films.

The transmission curves show that transmittance is relatively low (below 40%). The curves reveal that Cu_2S thin films are less transparent. Comparable results were obtained by Parreira *et al.* (2010) as having a transmittance of 42%. In the shorter wavelength, transmission is caused by interband transitions from valence band to the conduction band. The higher wavelength region the transmission is as a result of free carriers (Saadeldin *et al.*, 2014). Transmission is higher at lower concentrations (0.1M, 0.2M, and 0.3M) of copper, while at the same time, a substantial decrease of transmission is found in higher concentrations (0.4M and 0.5M) with the exception of 0.6M where transmittance was higher due to in-homogeneous structure of thin film surface due to rapid uncontrolled precipitation or hydrolysis in the solution (Isah *et al.*, 2008). This is explained by incomplete nucleation step with irregular growth rate of the thin film. Therefore the optimum molar concentration of 0.5M that gave the lowest transmittance was selected to deposit p-type Cu_2S thin films for solar cell application. The Cu_2S is a poor transmitter of photons incident on the film but a good absorber.

5.2.2 Reflectance

Figure 5.2 shows the reflectance spectra of Cu_2S for the wavelength between 300-1200nm. It is observed that the thin film with least (0.1M) concentration of copper (II) ions reflects more light as shown (about 11%) whereas the thin film with highest concentration (0.6M) has least reflectance of about 7%. Reflectance spectra show that Cu_2S is poor reflector because the low percentage reflectance between 7 and 11%. The film thickness of copper (II) ions increases with increase in the concentration of copper (II) ions in the substrate (Isah, 2008; Oloomiet *et al.*, 2010).

The resulting reflectance shows that the Cu_2S thin films deposited are poor reflectors of light therefore suitable for p-type material for solar cell applications (Osoro, 2011). There is sharp decrease of reflectance above 500 nm wavelength for all thin films. This observation can be explained as a result of high transmission of photons. The peak observed is associated with

interband transition where electrons from filled states at the top of valence are excited to empty states in the conduction band. This photo-transition causes sharp peak at low energy ranges is referred to as fundamental absorption (Osoro, 2011).

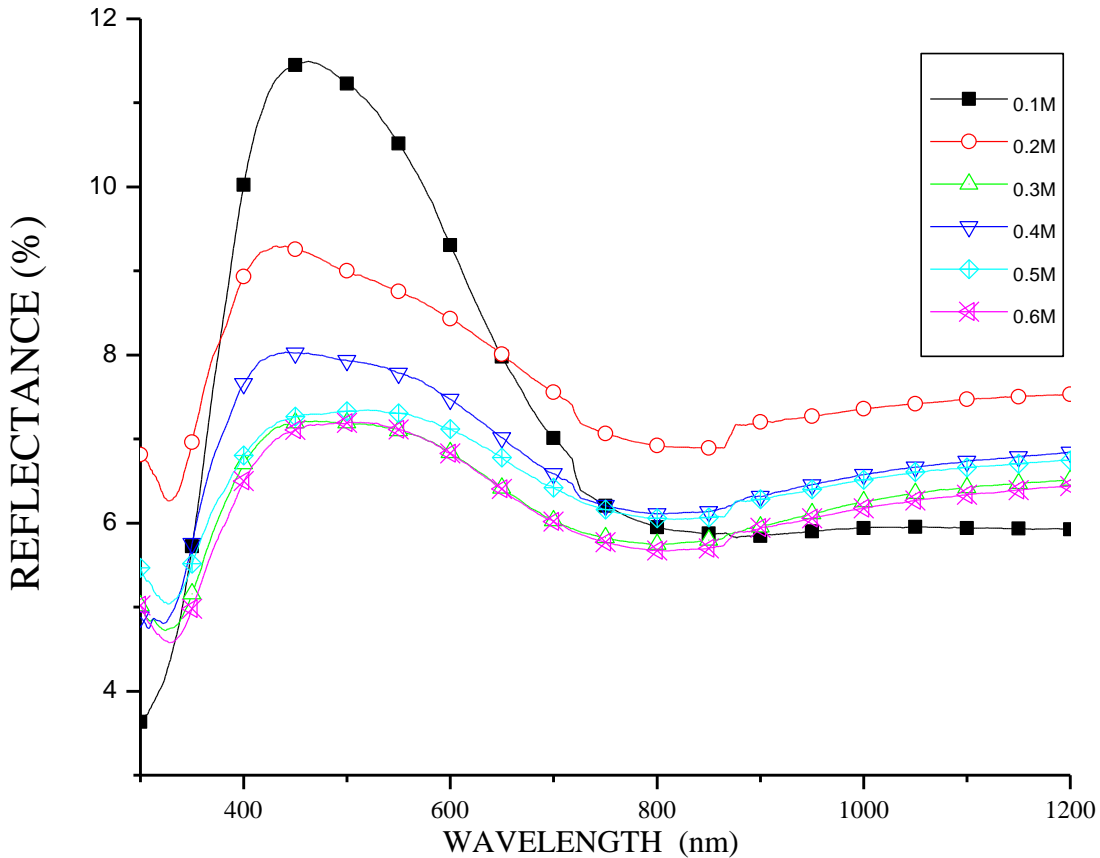


Fig. 5.2 Reflectance (R) as a function of wavelength (λ) for Cu_2S thin films

5.2.3 Absorbance

The absorbance spectra in fig 5.3 show that absorbance of Cu_2S thin film deposited from molar concentration of 0.5M is well above 75% thus the Cu_2S is a good absorber of photons. The variations observed may be due to dislocations on the surface of the thin film. However, observation reveals that absorbance increased as concentration of copper ions increased. This is

consistent with (Saaldilnet *al.*,2014).Kassim (2010) and Isah(2008)recommended that materials with high absorbance can be used as photoactive thin film materials and photochemical cells.

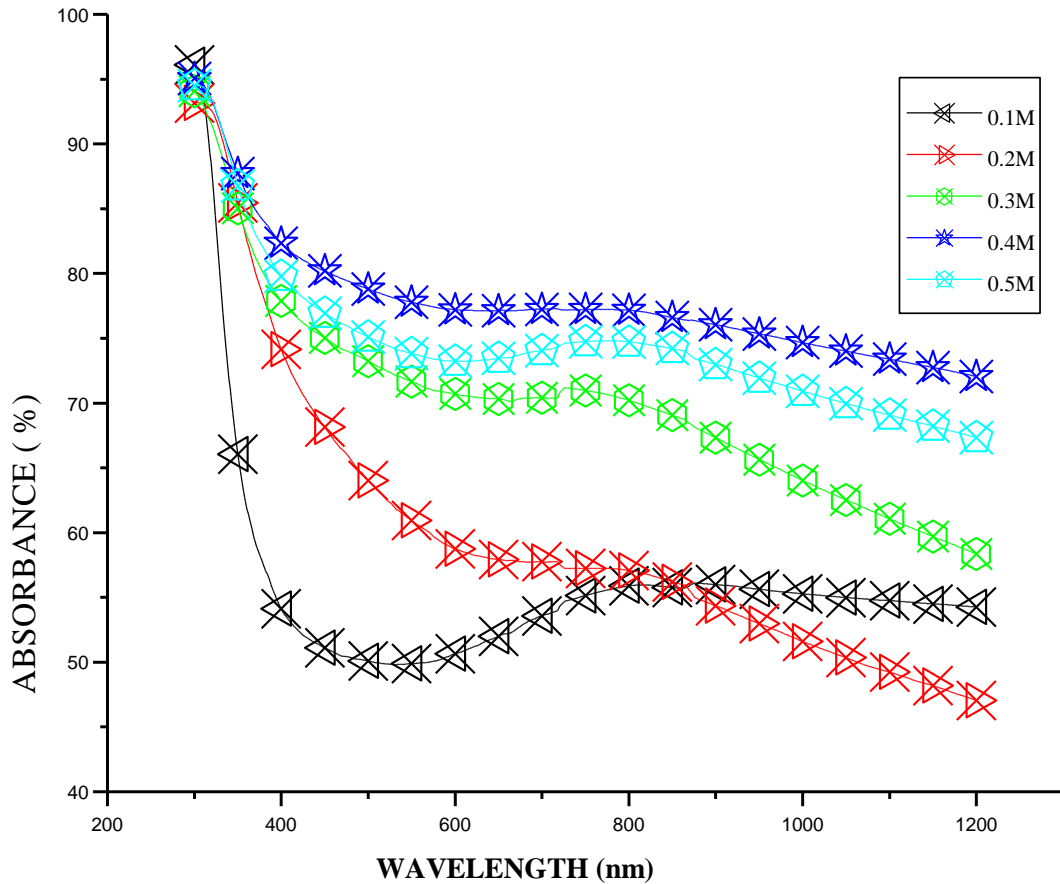


Fig. 5.3 Absorbance (A) as a function of wavelength (λ) for Cu_2S thin films.

5.2.4 Refractive index (n)

Figure 5.4 shows variation of refractive index with molarity of copper ions/thickness of the Cu_2S deposited film. It was observed that refractive index is between 1.62 and 2.01. It was also observed that Cu_2S thin film of lower thickness has relatively low refractive index value and the film with such low refractive index value possibly can be applied in antireflection coatings and solar cells (RamyaandGanesan, 2011).

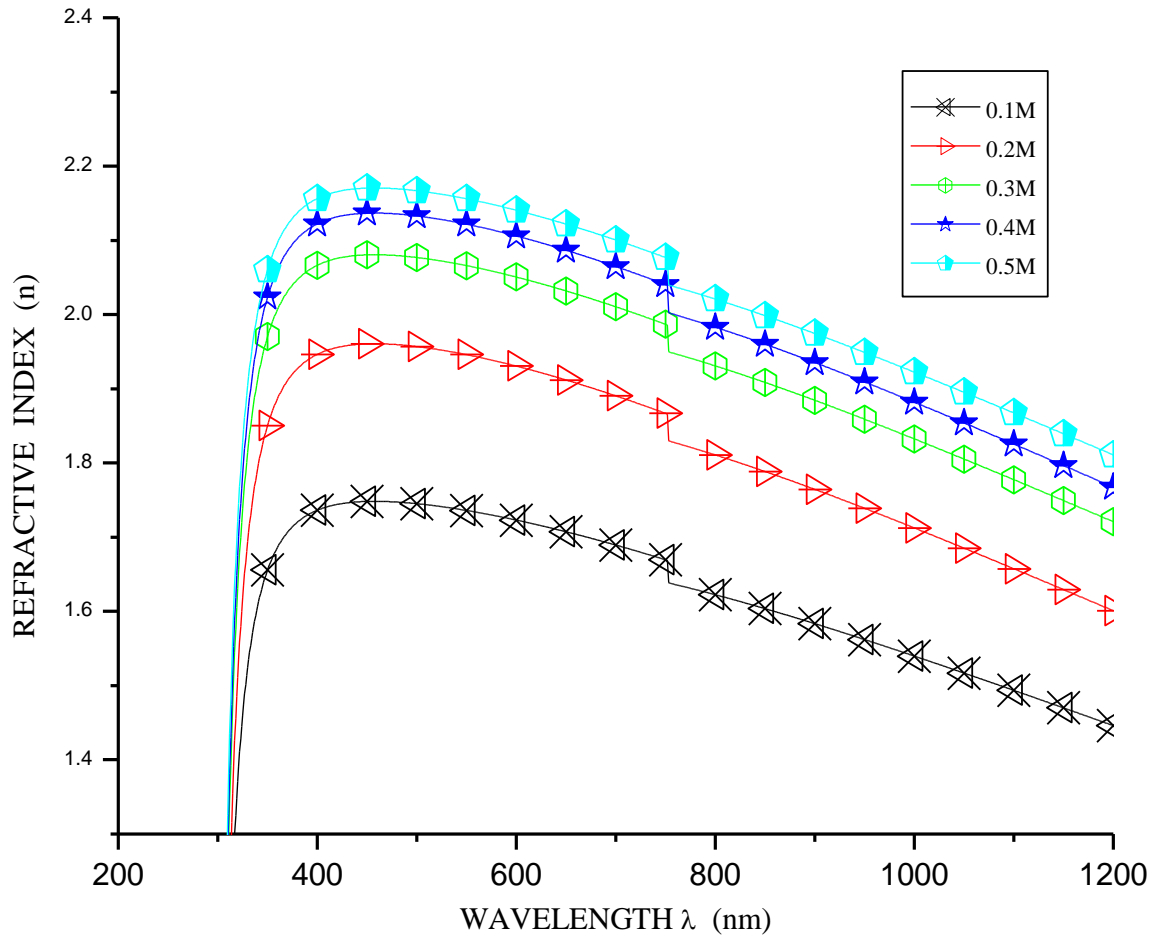


Fig. 5.4 Refractive index (n) as a function of wavelength (λ) for Cu_2S thin films

5.2.5 Band gap

Figure 5.5 shows variation of $(\alpha h\nu)^2$ against Energy ($h\nu$) between wavelength. The energy band gaps of Cu_2S were obtained by plotting $(\alpha h\nu)^2$ against energy ($h\nu$) and by extrapolating the linear part of the curve. The band gaps obtained were tabulated in Table 5.1. The results indicate that energy gap decreases with increase in film thickness. The decrease in the band gap is due to existence of internal electric field with defect in the film, increase in grain size due to recrystallization of smaller particles, Rajiet *al.*(2005) and Isacet *al.*(2007) have reported layers of Cu_xS with direct band gap varying from 2.66 to 3.0 eV. Thickness dependence of band gap can

arise due to the large density of dislocations and height of the crystalline films(RamyaandGanesan, 2011;Shindeet al., 2012).

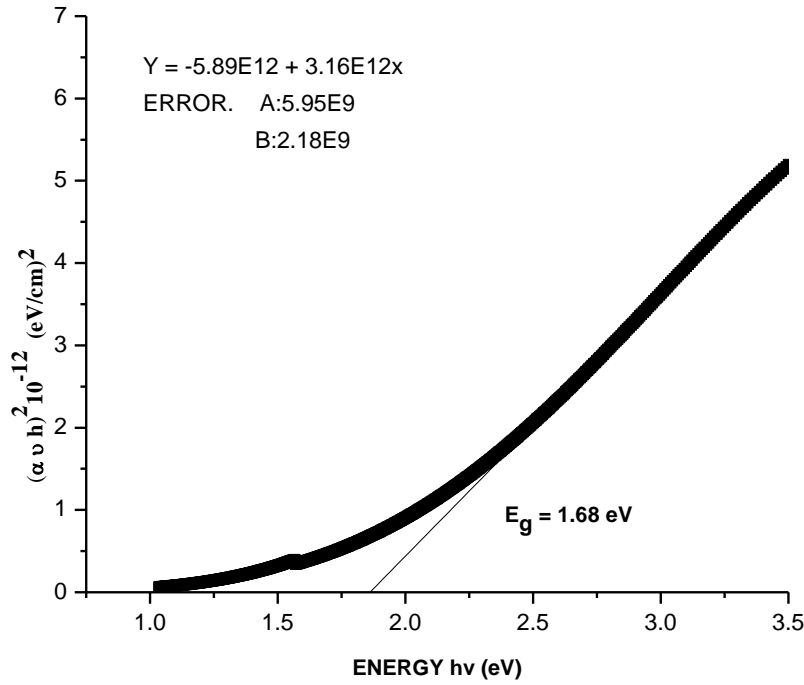


Fig. 5.5 Plot of $(\alpha h\nu)^2$ as a function of photon energy ($h\nu$) for 0.5M Cu₂S thin film.

The plots observed are linear over a broad range of photon energies confirming the direct type of transitions. The extrapolations of these plots on the energy axis give the value of the energy band gap of $1.68\text{eV} \pm 0.00285$. The linear part takes the form of $y = mx+c$ with a linear equation of $Y = 5.89\text{E}12 + 3.16\text{E}12x$.

Table 5.1 shows the Energy Gaps obtained of different film thickness. The Energy gap of the thin film number six (0.6M) is significantly higher due to rapid uncontrolled precipitation in the solution (Isahet al., 2008). This is explained by incomplete nucleation step with irregular growth rate of the thin film. The thin film number 5 was selected as the best choice because of its least energy gap(Isahet al., 2008).

Table 5.1 Energy gaps of copper (II) ions of different thickness

THIN FILM NO.	CONCENTRATION OF Cu ²⁺ ions	ENERGY GAP (eV)	FILM THICKNESS (nm) Error: ±0.5
1	0.1M	2.24 ± 0.00380	300
2	0.2M	1.92± 0.00389	305
3	0.3M	1.88 ± 0.00295	307
4	0.4M	1.84± 0.00608	310
5	0.5M	1.68 ± 0.0085	326
6	0.6M	2.64 ± 0.00316	350

5.2.6 Absorption coefficient

The variation of absorption coefficient with wavelength is illustrated in the figure 5.6

It was observed that absorption was highest at lower wavelengths. Good absorbers have high absorption coefficients consequently, exciting electrons into the conduction band. Table 5.2 shows listed average absorption coefficients which fall between 10^4 to 10^5 cm⁻¹ in the wavelength range 300-1000nm. Mosiori (2012) reported similar values within the desirable absorber materials for solar cell applications.

Table 5.2. Absorption coefficients of copper (II) ions of different wavelengths

Concentration of Cu ²⁺ ions	0.1	0.2	0.3	0.4	0.5	0.6
Average Absorption Coefficient [(x 10 ⁵)(cm ⁻¹)]	4.28	1.72	2.13	2.03	0.04	2.30

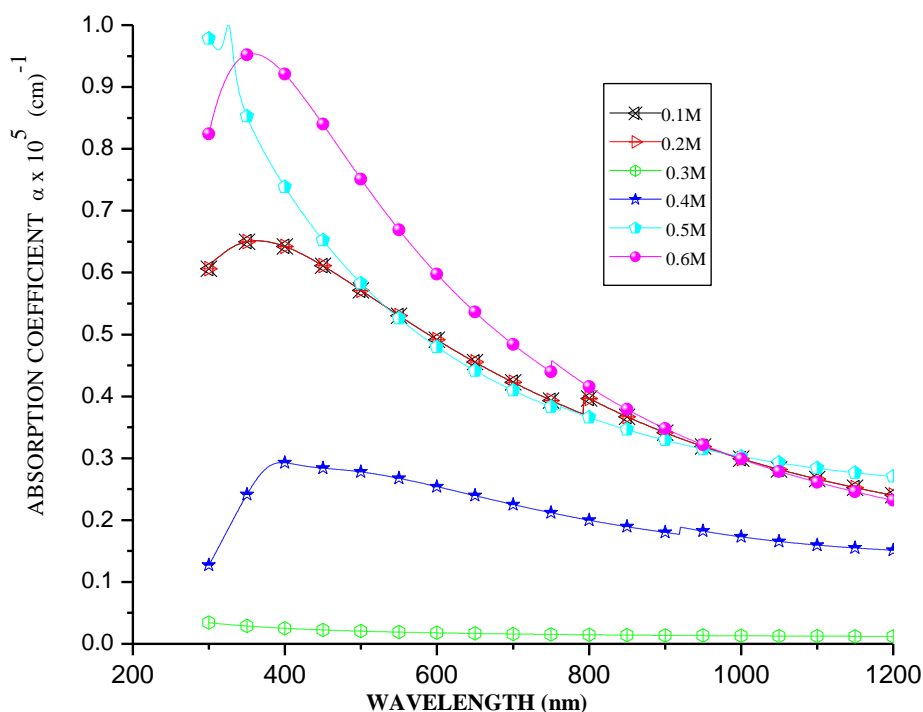


Fig 5.6 Plots of Absorption coefficient (α) as a function of wavelength (λ) of Cu_2S thin films.

5.3. Electrical Properties of p-type Cu_2S

The resistivity of Cu_2S thin films were analyzed using four point probe method. Fig 5.7 shows variation of resistivity and conductivity with molarity of copper (II) ions. Resistivity was observed to decrease with increase in the concentration of copper ions. The resistivity decrease can be attributed to the increase in carriers' concentration and their mobility. Nair and Nair (1989) reported similar results of conductivities ranging between 1.38×10^{-1} to $1.23 \times 10^{-7} (\Omega/\square)^{-1}$ were obtained by (Buba and Adelabu, 2009).

Table 5.3: Electrical properties of p-type Cu₂S

Copper (II) ions concentration	Electrical Resistivity (Ω/\square) ± 0.5 Error	Conductivity($\sigma \times 10^{-3}$) [$\Omega\text{-cm}$] ⁻¹ Error: ± 0.0005	Thin Film Thickness (nm) ± 0.05 Error
0.1M	479	2.09	300
0.2M	303	3.30	305
0.3M	241	4.15	307
0.4M	167	5.99	310
0.5M	86	11.6	326
0.6M	87	11.0	350

Table 5.3 shows how the electrical resistivity and conductivity varies with the thickness of the Cu₂S thin films. Electrical resistivity decreases with the increase in thickness of the thin films. This is due to the increase in both the carrier concentration of copper II ions and the grain size of the film at higher thickness (Ramyaand Ganesan, 2012).

Figure 5.7 is a plot of resistivity and conductivity of Cu₂S thin films against concentration of copper (II) ions. Resistivity varies inversely as conductivity. It is observed that the conductivity increases as resistivity decreases with increase in concentration of copper (II) ions. The copper rich film conducts electricity more than the copper deficient thin film. This is because of the electrical metallic properties of copper.

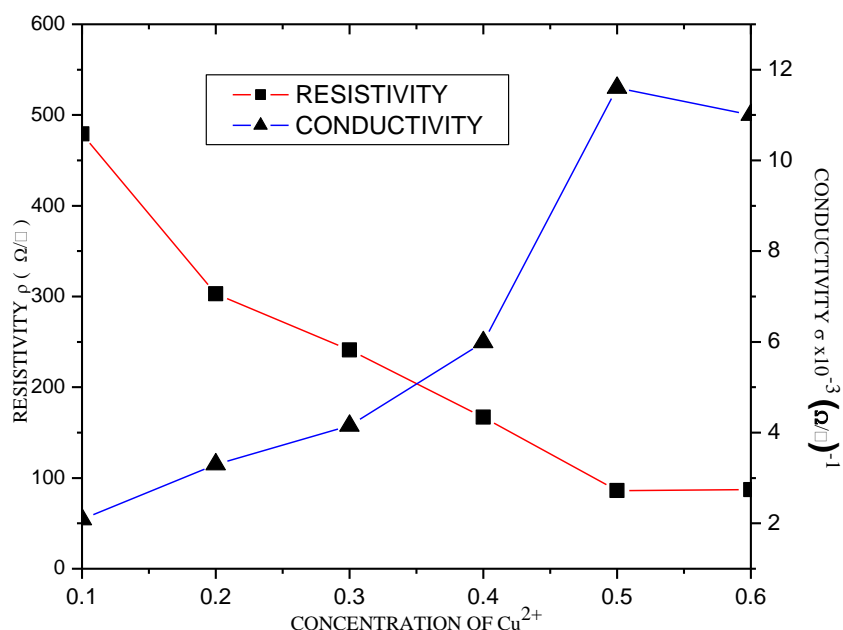


Fig 5.7: Electrical resistivity and conductivity varied with Concentration of copper ions

Table 5.4 gives a summary of optical and electrical properties of Cu₂S thin films. The thin films with 0.5 M concentration has the least band gap (1.68 ± 0.0085 eV) which makes it the best material for an active part of the solar cell.

Table 5.4 Summary of optical and electrical characteristics of Cu₂S thin films

Concentration	AV. T%	AV. A%	AV. R%	BAND GAP (eV)	Conductivity σ $\times 10^{-3} (\Omega/\square)^{-1}$
0.1M	38.47	72.83	7.31	2.24 ± 0.00380	2.09 ± 0.0005
0.2M	28.70	78.72	7.72	1.92 ± 0.00389	3.30 ± 0.0005
0.3M	20.56	62.97	6.29	1.88 ± 0.00295	4.15 ± 0.0005
0.4M	13.99	52.45	6.78	1.84 ± 0.00608	5.99 ± 0.0005
0.5M	7.03	75.46	5.76	1.68 ± 0.0085	11.6 ± 0.0005
0.6M	27.33	65.82	6.55	2.64 ± 0.00316	11.0 ± 0.0005

5.4 Optical properties of CdSeS

5.4.1 Transmission

Figure 5.8 shows transmission spectra of CdSeS variation with wavelength. The spectra reveal that CdSeS thin films exhibit high transmission above 70% in the range between 300nm and 1200nm wavelength. Isahet *al.* (2008) reported transmittance of about 80%. Mosiori (2012) reported CdS:Zn transmittance between 75% and 83% in the wavelength range between 200nm to 2200nm. It is observed that transmittance decreases as the concentration of Se increased. However, doping with 0.8 M selenium ions does not significantly reduce the transparency of the thin film. The Cd_{0.2}Se_{0.8}S thin film has transparency above 70% and a largest band gap which qualifies it to be a suitable window layer material. There is a decrease in transmittance at about wavelength of 550 nm. This can be explained by a possibility in increase in optical scattering due to uneven surface of the thin films (Osoro, 2011).

5.4.2 Absorbance

Figure 5.9 shows absorbance spectra of CdSeS. The spectra reveal that absorbance of CdSeS thin films obtained were below 25%. This indicates that the CdSeS thin films are poor absorbers. This is consistent with the characteristics of window layer materials (Singh and Bhushan, 2008; Ugwueta *al.*, 2007).

5.4.3 Reflectance

The figure 5.10 shows reflectance spectra of CdSeS thin films of varying concentrations of Selenium ions. It was observed that reflectance obtained from all films had reflectance values below 10%. It is seen from the spectral curves, doping of CdS with Se reduced its reflectivity properties. CdSeS being the n-type material of the solar cell, reflectivity is supposed to be as low as possible. This behavior of the spectra reveals the smooth reflectivity of surfaces. Therefore there is no much scattering loss at the surface (Osoro, 2011).

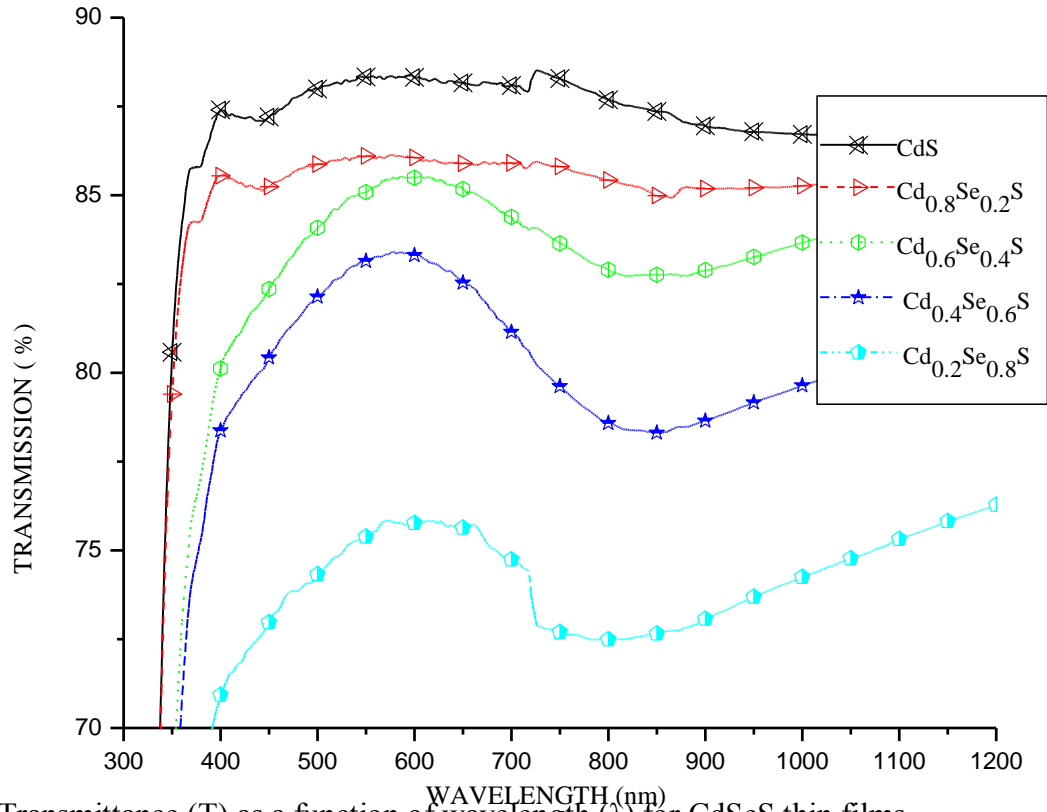


Fig. 5.8 Transmittance (T) as a function of wavelength (λ) for CdSeS thin films.

5.4.4 Extinction coefficients (k)

The variation of extinction coefficient with wavelength is illustrated in the figures 5.11

The figure shows that extinction coefficients are lowest within visible range of photon energy.

This is an indication that the CdSeS thin films deposited are suitable for High-quality window materials so as to minimize absorption losses (Mosiori, 2012). CdSeS has satisfied that requirement and thus suitable for photovoltaic applications as a window layer.

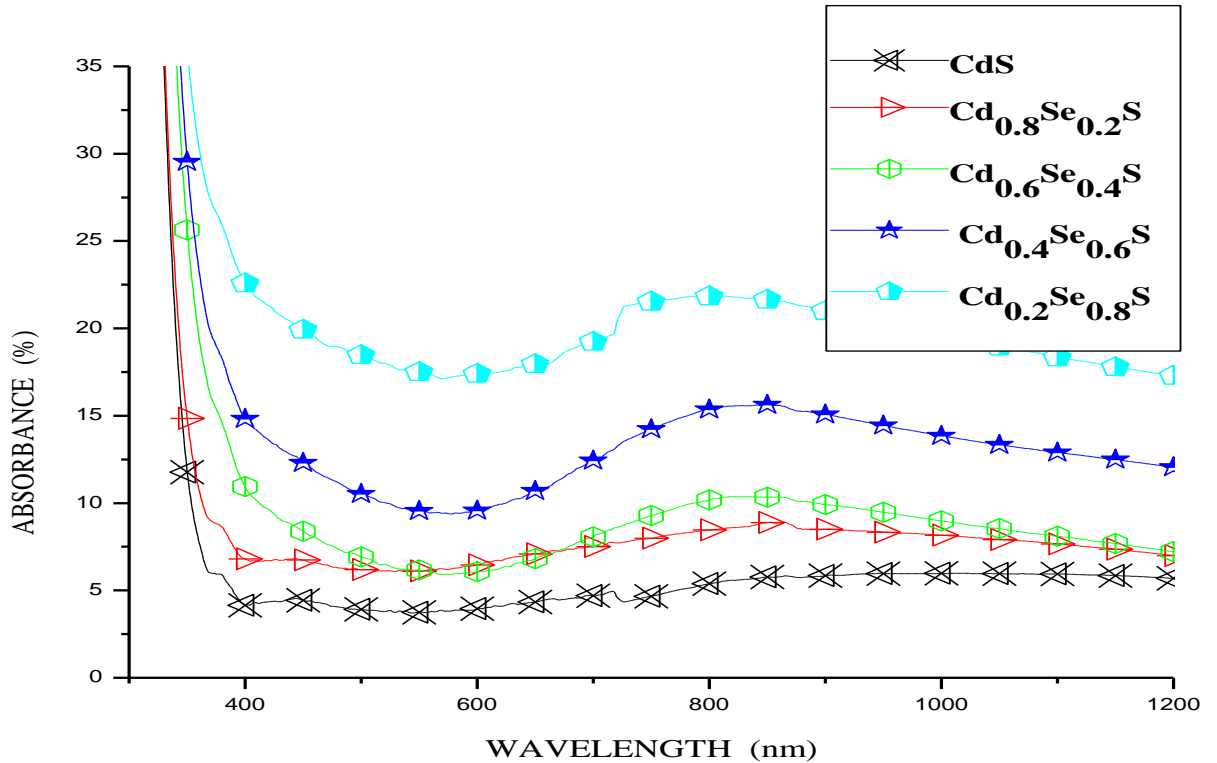


Fig. 5.9: Absorbance (A) as a function of wavelength (λ) for CdSeS thin films.

5.4.5 Absorption coefficient of CdSeS

Figure 5.12 shows CdSeS thin films absorption coefficients. The films showed very low absorption coefficients about $1.5 \times 10^4/\text{cm}$. Materials with low absorption coefficients do not readily absorb photons which are responsible for exciting electrons into the conduction band. The results obtained are consistent with the results of Osoro (2011) which indicates that the films with low absorption coefficients are optically transparent to photons incident on their surface. The values of absorption coefficient between 1eV and 4eV of CdSeS are below $0.2/\text{cm}$ within the visible spectrum energy range (300 – 1200nm) indicating that the films are transparent at low energies. This is for the reason that electrons are not excited from the valence band to conduction band at low energies.

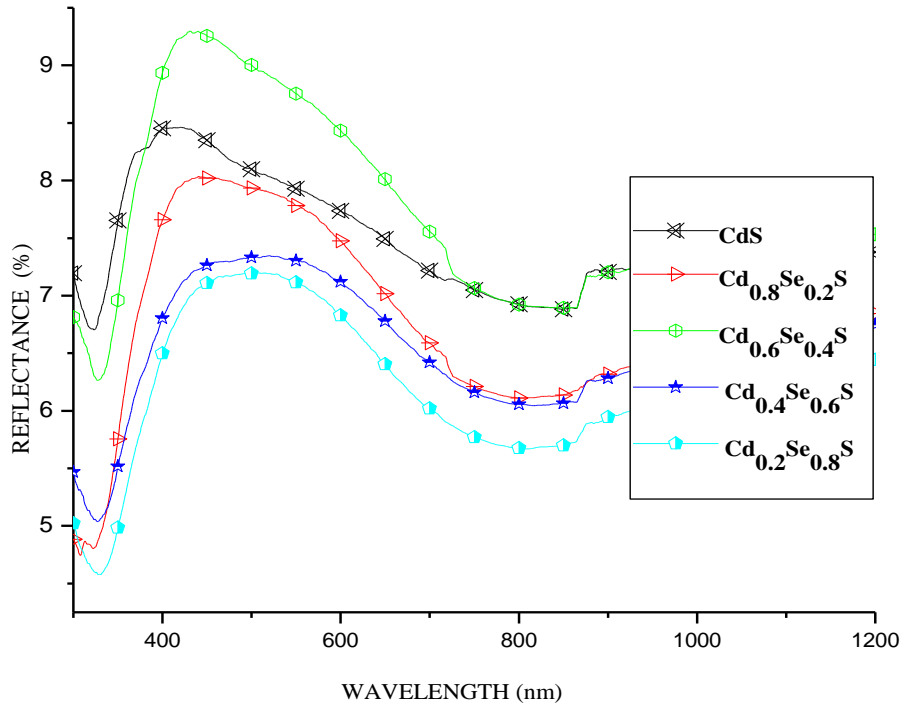


Fig. 5.10 Reflectance (R) as a function of wavelength (λ) of CdSeS thin films.

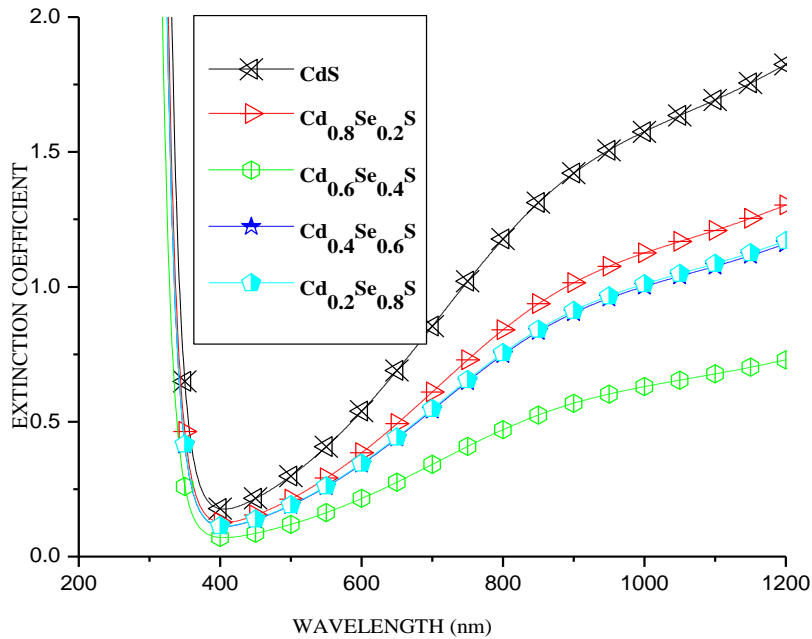


Fig. 5.11 Plots of

Extinction coefficient (k) as a function of wavelength (λ) for CdSeS thin films.

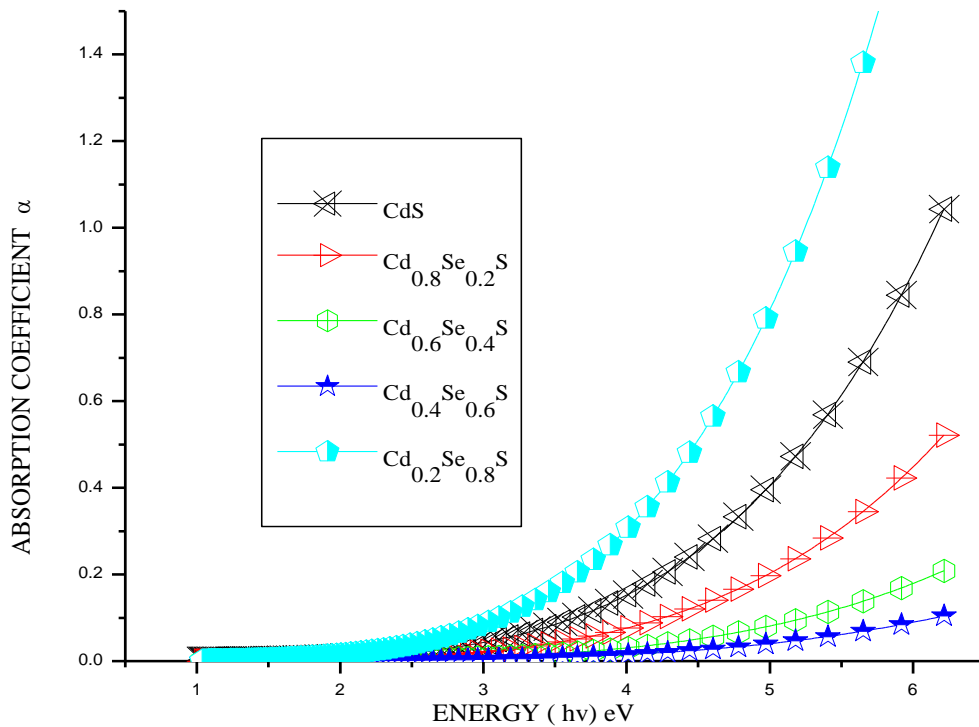


Fig.5.12 Plots of Absorption Coefficient (α) as a function of energy (eV) for CdSeS thin films.

5.4.6 Refractive index of CdSeS

Fig 5.13 illustrates how refractive index of CdSeS thin films varies with wavelength between 300 and 1200nm. It is observed that refraction index (n) decreases with increase Se concentration. It is also observed that the thicker the film the higher the refractive index. The refractive index obtained varies between 1.35 and 2.2. The values obtained are within the reported values ranging from 2.39 to 2.55 in the wavelength range between 200 and 2200 nm of CdS:Zn (Mosiori, 2012). The experimental results indicate that at higher photon energies radiation is less refracted and thus the characteristic of n-type window material suitable for solar cell applications.

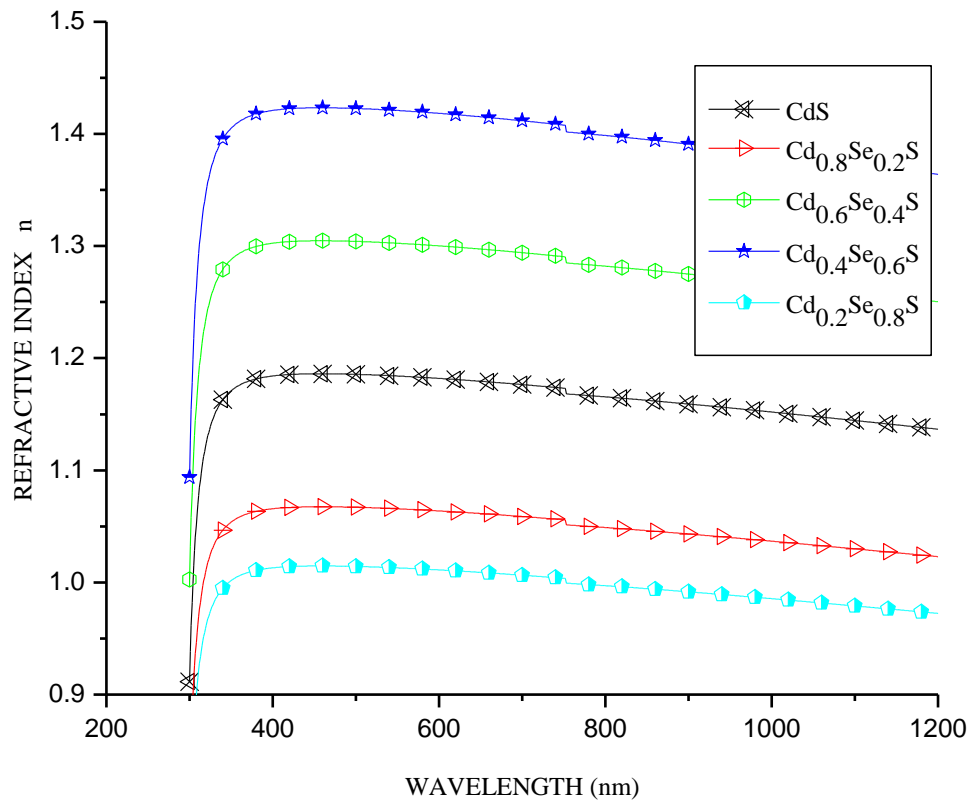


Fig 5.13 Refractive index (n) as a function of wavelength (λ) for CdSeS thin films.

5.4.7 Di-electric constant of CdSeS

Fig 5.14 shows variation of real dielectric constant of CdSeS as a function of frequency for different thickness. Thin films with low dielectric constant experience minimal recombination losses and less interference on movement of charge carriers (Mosiori, 2012). Higher dielectric constant contributes to high retention of electrons and holes thereby increasing probability of recombination (Mosiori, 2012).

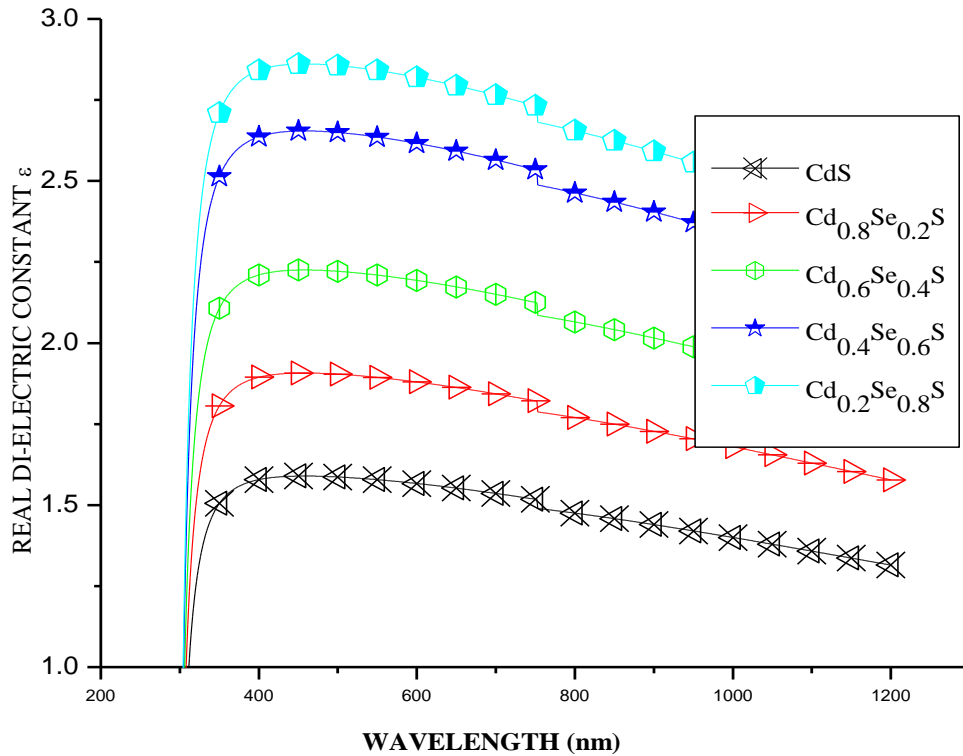


Fig 5.14 A plot of Real di-electric constant of CdSeS against wavelength of varying concentrations

5.4.8 Optical energy band gap of CdSeS

Energy band gaps of CdSeS thin films were obtained by plotting $(\alpha h\nu)^2$ against photo energy $(h\nu)$. Extrapolating the linear part of the curve as shown in the figure 5.15, reveals that energy band gaps varied in proportion with film thickness.

Table 5.4 shows the obtained values of energy band gaps which decreased with increase in film thickness. Internal electric field and defects in the thin films contribute to the decrease in the band gap. Increase in grain size due to recrystallisation of smaller particles (Rajiet *al.*, 2005). Thin film with highest band gap was selected for solar cell application due to its suitable window layer properties like optical transparency and high bad gap.

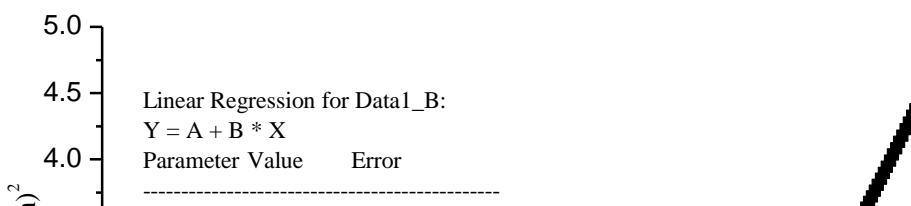


Fig. 5.15 Plot of $(\alpha h\nu)^2$ as a function of energy ($h\nu$) for 0.8M $\text{Cd}_{0.2}\text{Se}_{0.8}\text{S}$.

Table 5.5: Energy gaps of CdSeS thin films of different thickness

Formulae	Band gap (eV)	Film thickness (d) (nanometers)
CdS	2.640 ± 0.0821	356.1 ± 0.05
$\text{Cd}_{0.8}\text{Se}_{0.2}\text{S}$	2.924 ± 0.0209	300.6 ± 0.05
$\text{Cd}_{0.6}\text{Se}_{0.4}\text{S}$	2.970 ± 0.0209	305.5 ± 0.05
$\text{Cd}_{0.4}\text{Se}_{0.6}\text{S}$	3.091 ± 0.0222	306.5 ± 0.05
$\text{Cd}_{0.2}\text{Se}_{0.8}\text{S}$	3.314 ± 0.0081	340.1 ± 0.05

5.5 Electrical Properties of CdSeS

The sheet resistivity of CdSeS thin films were measured using four point probe method. The results are shown in the Table 5.5 and represented by figure 5.16.

Resistivity decreased as selenium ions concentration increased. Resistivity is a measure of metal lattice displacement from perfect regularity. Resistivity decreases with increasing film thickness which is in accordance with the results of semiconducting films in relation to charge scattering carriers (Saadel*netal.*, 2014). Increase in resistivity is attributable to surface of the film with lot of empty spaces that creates grain boundaries resulting in increase in resistivity (Ubale*etal.*,2011).

Table 5.6 Electrical properties of CdSeS

FORMULAE	ELECTRICAL RESISTIVITY (Ω/\square) ± 0.5 error	Conductivity [Ω/\square] ⁻¹ Error: ± 0.00005	THIN FIM THICKNESS (nm) ± 0.05 error
Cd _{0.8} Se _{0.2} S	175.54	0.00570	300.6
Cd _{0.6} Se _{0.4} S	165.53	0.00604	305.4
Cd _{0.4} Se _{0.6} S	150.24	0.00664	306.5
Cd _{0.2} Se _{0.8} S	130.78	0.00765	340.2
CdS	135.86	0.00736	356.1

It was observed that the cadmium rich thin films have lowest conductivity which increases with increasing selenium ions as dopant to a maximum concentration of selenium of 0.8M. Therefore, it is observed that increasing selenium concentration as a dopant improves conductivity. Figure 5.18 shows that Selenium concentration of 0.85M (optimum) obtained by setting the derivative

of $Y = 208.92 - 162.5x + 94.7x^2$ to zero. The resistivity of the CdSeS obtained is about $140.8 \Omega/\square$ as per the optimum value obtained by polynomial fit of resistivity of CdSeS.

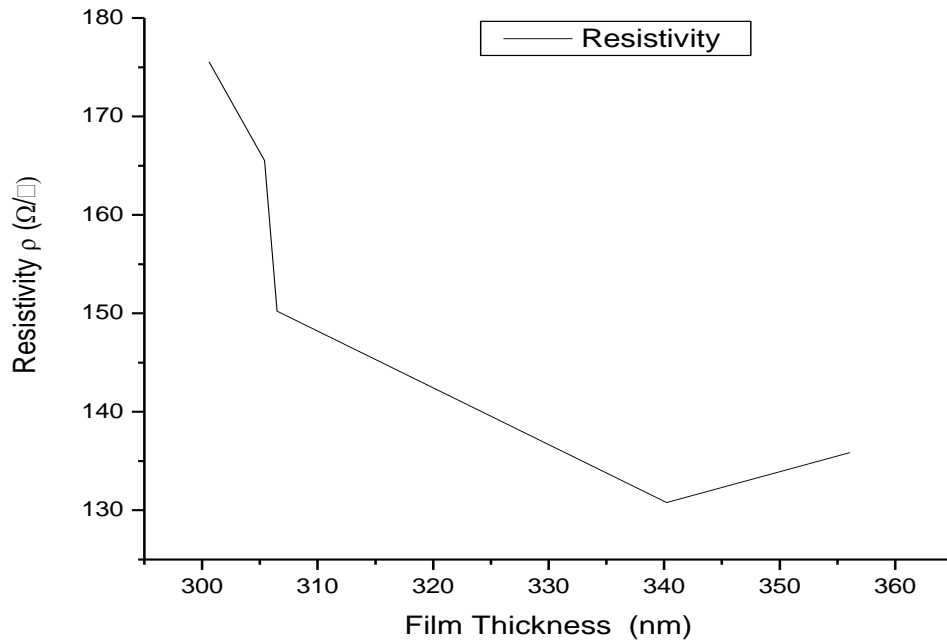


Fig 5.16 A graph resistivity against thin film thickness of CdSeS

Table 5.7 gives a summary of optical and electrical properties of CdSeS as a window material for solar cell applications. A window material should have high transmittance which allows maximum photons to excite electrons from valence band to conduction band. The reported values of Energy gap and resistivity are within the recommended range of desirable window layer materials.

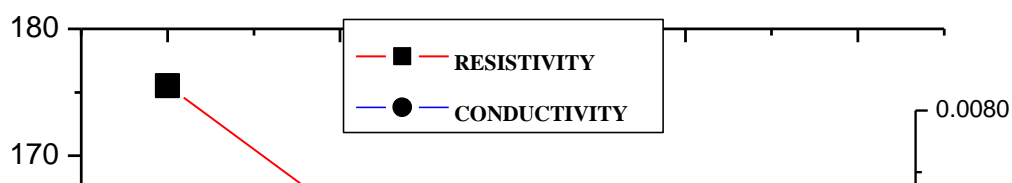


Fig. 5.17: Resistivity and conductivity of $\text{Cd}_{0.2}\text{Se}_{0.8}\text{S}$ as a function of concentration of Selenium ions.

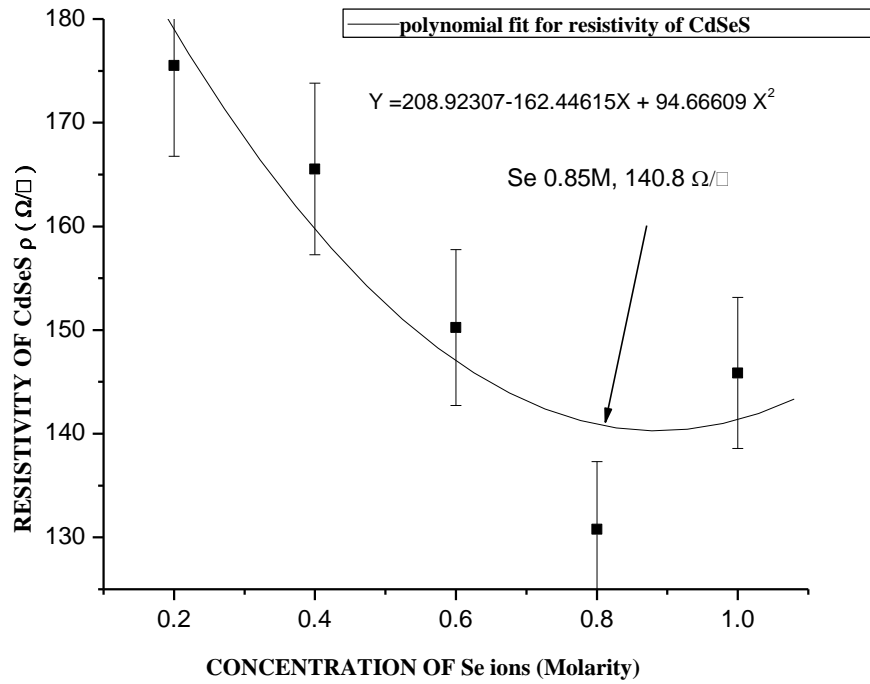


Fig. 5.18 Optimization of resistivity of CdSeS thin films

Table 5.7 Summary of opto-electric properties of CdSeS

PROPERTY	CdS	Cd _{0.8} Se _{0.2} S	Cd _{0.6} Se _{0.4} S	Cd _{0.4} Se _{0.6} S	Cd _{0.2} Se _{0.8} S
TRANSMISSION %	87.8	85.6	83.4	80.9	73.6
ABSORBANCE %	4.4	7.1	8.3	12.3	19.8
REFLECTANCE %	7.8	7.3	8.3	6.9	6.6
ENERGY GAP (eV)	2.640	2.924	2.970	3.091	3.314
ERROR ($\pm eV \times 10^{-2}$)	± 0.0821	± 0.02097	± 0.02088	± 0.02222	± 0.0081
RESISTIVITY ($\pm 0.005 \Omega/\square$)	135.86	175.54	165.53	150.24	130.78

5.6 Optimized opto-electric properties for solar cell application

The optimum concentrations that gave best properties suitable for solar cell fabrication were selected for application.

5.6.1 n-type window layer

Cd_{0.2}Se_{0.8}S thin film was selected to fabricate solar cell because of its largest gap energy (3.314 eV) as obtained in figure 5.15 and tabulated in Table 5.7. This film is a good transmitter (between 73.6 and 85.6%), a poor reflector (between 6.6 – 7.3 %). It's a poor absorber (between 7.1 and 19.8%) whose resistivity is between 130.78-175.54 Ω/\square thus one of the best n-type semiconductor materials.

5.6.2 P-type absorption layer

Table 5.4 gives the summary of Cu₂S thin films characteristics. Thin film deposited in 0.5M solution was chosen because of its poor transmittance (7.03 %), poor reflectance (5.76 %), good absorbance (75.46 %) and the best band gap (1.68 eV \pm 0.0085).

Silver paste was used as the contact. I-V characteristics were determined by the solar cell simulator and the results tabulated in Table 5.8 and the results were used to plot aI-V characteristic and power output curve in figure 5.18.

5.7 Solar cell I-V Characteristics

Table 5.8 presents the obtained voltage and current from the solar cell simulator. Figure 5.18 represents current voltage characteristic of the fabricated $Cd_{0.2}Se_{0.8}S/Cu_2S$ solar cell.

The open circuit voltage ($V_{OC} = 0.40V$), represents the maximum voltage obtainable from the cell, which occurs at zero current and short circuit current ($I_{sc} = 0.0039A$) is the maximum current obtained from the cell at zero voltage. The maximum power ($P_{MAX} = 0.00094W$) obtained as a product of maximum current ($I_{MAX} = 0.0036A$) and maximum voltage ($V_{MAX} = 0.26V$) as shown in the Figure 5.18.

5.8 Solar cell fill factor (FF) and conversion efficiency (η)

Fig 5.18 is a plot of I–V characteristics of $Cu_2S/CdSeS$ solar cell illuminated at 25^0C . The measured values are as follows: $I_{SC} = 0.0039A$, $V_{oc} = 0.4V$, $I_{max} = 0.0036A$ and $V_{max} = 0.26V$. From the data obtained, the Fill Factor was obtained using the equation 5.1 as:

$$FF = \frac{P_{max}}{V_{oc} I_{sc}} \quad (5.1)$$

$$FF = \frac{P_{max}}{V_{oc} I_{sc}} = \frac{0.0036 \times 0.26}{0.4 \times 0.0039} = \frac{0.000936W}{0.0039 \times 0.4} = 0.6$$

Solar cell energy conversion efficiency was obtained as:

$$Efficiency \eta = \frac{P_{OUT}}{P_{IN}} \times 100 = \frac{0.000936W}{1000W/m^2 \times 1.16 \times 10^{-4}m^2} \approx 0.81\%$$

Where P_{IN} (power in) = $E \times A_c$

$$= (1000\text{W/m}^2) \times (1.16 \times 10^{-4} \text{m}^2)$$

$$= 0.116\text{W}$$

P_{max} or $P_{\text{OUT}} = (0.000936\text{W})$

Table 5.8 The I-V characteristics of the CdSeS/Cu₂S solar cell under illumination

VOLTAGE (V)	CURRENT ($\times 10^{-3}$ A)	POWER OUT ($\times 10^{-4}$ W)
0	3.9 = I_{SC}	0
0.04	3.9	1.56
0.09	3.9	3.51
0.15	3.9	5.85
0.26 = V_{MAX}	3.6 = I_{MAX}	9.36 = P_{MAX}
0.29	3.2	9.28
0.31	2.9	8.99
0.32	2.5	8.00
0.34	2.0	6.80
0.35	1.6	5.60
0.36	1.2	4.32
0.38	0.8	3.04
0.39	0.5	1.95
0.40 = V_{OC}	0	0

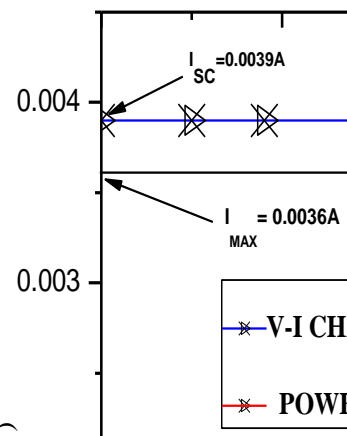


Fig. 5.18 plot of I-V characteristics of a solar cell

Alternatively,

$$\eta = \frac{I_{SC} V_{OC} FF}{E_{IRRAD} A_C} = \frac{0.0039 \times 0.4 \times 0.6}{1000 \times 1.16 \times 10^{-4}} = 0.0081 \approx 0.81\%$$

The low conversion efficiency of hetero-junction CdSeS/Cu₂S may be attributable to the higher series resistance which lowers values of FF and conversion efficiency. This occurrence was investigated by Saraf (2012) and Adurodija *et al.* (2005). Also the tendency of hetero-junction towards numerous recombination centers positioned in the p-n junction might have contributed to the low conversion efficiency of this solar cell Saraf (2012). In addition, lattice mismatch

between the pair of junctions which are related to substrate preparation procedure and the formation process contributes to lower V_{OC} and FF (Ashouret *et al.*, 2005).

Many researchers fabricated solar cells whose efficiencies were lower than 12%. Wu *et al.* (2008) fabricated CdS/Cu₂S solar cell which had V_{oc}=0.6mA, I_{sc} =5.63mA/cm² , η = 1.6% and FF=

0.474. Saraf (2012) obtained efficiency between 1.472% and 10.9% of a CdS/Cu₂S solar cells on various substrates. The following parameters were measured $V_{oc} = 0.58V$, $I_{max} = 5.1mA$, $I_{sc} = 0.0058A$ and $V_m = 0.48$, $FF = 0.73$ and $P_{max} = 2.45mW$.

CHAPTER 6

CONCLUSIONS AND RECOMMENDATIONS

6.1 Conclusions

CdSeS and Cu₂S thin films were effectively deposited on glass substrates by chemical bath deposition method. The optical and electrical properties of the thin films were investigated. The energy band gaps, transmittance, reflectance, resistivity and absorption measurements of thin films that gave optimum properties were selected to fabricate a solar cell.

Transmission of CdSeS thin films was above 73 % in the visible range. Reflectance obtained was below 8 % and absorbance below 19 %. The band-gap range was between 2.64eV to 3.314eV. Cd_{0.2}Se_{0.8}S gave the highest value (3.314eV). Refractive index and dielectric constants increased with concentration of the Se ions. Resistivity of the film decreased with increase in Se ions concentration from 130.78 to 175.54 Ω/\square . This was as a result of metalloid properties of Selenium. Cd_{0.2}Se_{0.8}S films were found to be having the best window (n-type) material.

Cu₂S was found to be a poor transmitter (7 to 38 %), poor reflector (6 % to 7 %) and good absorber (52.45 to 78.72%). Band gaps varied between 1.68 to 2.64eV. Band gaps decreased with increase in the concentration of copper (II) ions. Resistivity varied between 86 to 184 Ω/\square . Thus the Cu₂S (0.5M) was found to have the optimum conditions for an absorber (p-type) material. Energy gap of Cu₂S thin film that was selected had a value of 1.68eV and conductivity of 11.6×10^{-3} (Ω/\square).

The best combination of both thin films (Cu₂S and CdSeS at 0.5 M and 0.85 M concentrations respectively) were selected to fabricate a Cd_{0.2}Se_{0.8}S/Cu₂S solar cell whose short circuit current $I_{sc} = 0.0039A$, open circuit voltage $V_{oc} = 0.40V$, maximum voltage $V_{max} = 0.26A$, maximum current $I_{max} = 0.0036A$, maximum power $P_{max} = 0.00094W$, fill factor $FF = 0.602$ and conversion

efficiency of 0.81%. In view of the above reported characteristics of the solar cell, it was concluded that the materials chosen can be suitably used to improve the output of the solar cells.

6.2 Recommendations

Considering low conversion efficiency of the solar cell, the following recommendations are proposed:

- i. Further investigation to be done to determine whether the annealing of thin films in a vacuum could improve the conversion efficiency of the cell.
- ii. Using Ethylenediaminetetraacetic acid (EDTA) as a complexing agent could improve the optical properties of the thin films like energy band gap (E_g).
- iii. Fabricated CdSeS/Cu₂S solar cell can be adopted to supply low current to micro-power comparator devices that require supply current of 300 nA.

REFERENCE

- Abdullah, S. (2007).** *Preparation and Characterisation of chlorine doped cadmium sulphide Thin Films and their Applications in Solar cells.* M.Sc thesis, Kings University. Saudi Arabia.
- Adurodija, F.O. and Carter, M.J. (2005).** *Fabrication and Characterization of CuInSe₂ Thin Film Solar Cells By Stacked Elemental Layer (SEL) Technique.* Newcastle. University of Northumbria.
- Al-Ayashi, W. M. (2007).** *Influence of annealing on the optical and electrical properties of chlorine doped CdS thin films and their Applications.* (Master's Thesis). King Saud University. Saudi Arabia.
- Altosaar, M., Ernits, K., Krustok, J., Varema, T., Raudoja, J. and Mellikov, E. (2004).** Comparison of CdS films deposited from chemical baths containing different doping impurities. *Journal of Thin Solid Films*, **480**, 147-150.
- Amanullah, F., Al-Shammari, A.S. and Al-Dhafiri, A. (2005).** Co-Activation effect of chlorine on the physical properties of CdS thin films prepared By CBD technique for Solar applications. *Journal of physica status solidi A (Applied Research 202)*, **13**, 2474-2478.
- Armin, G. (2009).** Thin-film solar cells. *Thin Solid Films*. **517**, 4706-4710.
- Ashour, A. (2006).** The Physical Characteristics of Cu₂S/CdS Thin-Film Solar Cell. *Journal of Optoelectronics and Advanced Materials*, **8**, 1447 – 1451.
- Ashour, A., Ramadan, K., El-Hady, A. and Akl, A.A.S. (2005).** Preparation and Characterization of The Junction CuInSe₂/CdTe Solar Cell By Stacked Elemental Layer (SEL) Technique. *Journal of Optoelectronics and Advanced Materials*, **7**, 1493-1498.
- Bayhan, H. (2006).** Tunneling-Enhanced Recombination in Polycrystalline CdS/CdTe Solar Cells. *Turkish Journal of Physics*, **30**, 109-114.
- Born, M. and Wolf, E. (1999).** *Principles of Optics* (7th Ed.). Cambridge University Press: Cambridge.
- Boyle, G. R. (1996).** *Renewable energy: Power for a sustainable future.* Oxford University Press, New York.
- Brendel, R. and Queisser, H. (1993).** The thickness dependence of open circuit voltages of p-n junction solar cells. *Sol. Energy Mater. Sol. Cells*, **29**, 397.
- Buba, A.D.A. and Adelabu, J.S.A. (2009).** Electrical conductivity of Cu_xS Thin films deposited by Chemical Bath Deposition (CBD) Technique. *Nigerian Journal of Basic and Applied Science*, **17**, 161-165.

Chaliha,S., Borah,M.N., Sarmah, P.C. and Rahman,A. (2008). Effect of substrate temperature on structural properties of thermally evaporated ZnSe thin films of different thickness.*Journal of Physics Conference Series*,**114**, 1.

Choi,Y., Young K.K., Jae-Eun, P., Hae, Y. and Kim, K. (2003).Improved transmittance in one dimensional metallic photonic crystals. *Physics of Condensed Matter*,**338**, 132-135.

Dharmadasa, I., Bingham, P., Echendu, O., Salim, H., Druffel, T., Dharmadasa, R., ... Abbas, A. (2014). *Fabrication of CdS/CdTe-Based Thin Film Solar Cells Using an Electrochemical Technique.* *Coatings*, **4**(3), 380–415. <http://doi.org/10.3390/coatings4030380>.

Dilli, Z. (2008). *Introduction to Device Physics*.University of Maryland, College Park.Retrieved from [www.ece.umd.edu/dilli/courses/enee 313](http://www.ece.umd.edu/dilli/courses/enee%20313).

DOE Office of Science.*Basic Research Needs for Solar Energy Utilization*, April 2005, available: <http://www.sc.doe.gov/bes/reports/list.html>.)

Fatehmulla, A., Al-Shammari, S. and Al-Dhafiri, A. M. (2014). Structural, Electrical and Optical Properties of Chlorine Doped CdS Thin films. *World Applied Sciences Journal*,**31**, 2073-2078publishing Association: New Jersey.

Goetzberger, A., Knobloch, J., Voss, B.(1998). *Crystalline Silicon Solar Cells: Technology and systems Applications*.John Wiley and Sons: New Jersey.

Gratzel, M.(2003).Dye sensitized solar cells. *Journal of Photochemistry and Photobiology*,**4**, 145-153.

Green, M. A. (2002). Third generation Photovoltaics: Solar cells for 2020 and beyond.*Journal of Physics*,**14**, 65-70.

Hegedus,S.S. (1997).Current-voltage analysis of a-Si and a-SiGe solar cells including voltage-dependent photocurrent collection.*Program Photovoltaic Applications*,**5**,151-168.

Henry, C.H.(1980). Limiting efficiencies of ideal single and multiple energy gap terrestrial solar cells.*Journal of Applied Physics*,**51**,4494–4500.

Hishikawa, Y.,Imura, Y. and Oshiro,T.(2000).*Irradiance dependence and translation of the I-V characteristics of Crystallines Silicon Solar cells*.28th IEEE Photovoltaic Specialists Conference.1464-1467.

<http://www.bp.com>. *Statistical Review of World Energy*, **2009**.

Isac, L. (2007). *Preparation and Characterization of Copper Sulphides Thin Films with Optoelectronics Applications.* Ph.D. Thesis,Universitatea din Bucuresti, Bucuresti,Romania.

Isah, K.U., Narayan, H., and Oberafo, A. (2008).Optimization of process parameters of Chemical Bath Deposition of Cd_{1-x}Zn_xS thin film.*Leonado Journal of Sciences*,**12**, 111-120.

Jain, A., Sagar, P., and Mehra, R. M. (2006). Band gap widening and narrowing in moderately and heavily doped n-ZnO films. *Solid-State Electronics*, 50(7-8), 1420–1424. <http://doi.org/10.1016/j.sse.2006.07.001>.

Johansen, L.G. (2004). *Basic semiconductor properties and the p-n junction*. (Msc. Thesis). University of Bergen.

Kassim, A., Nagalingam, S., Tee, T. W., Koon, K. L., and Min, H. S (2010). *Effect of pH value and electrolyte concentration on the copper sulphide thin films prepared by chemical bath deposition method*. Gazi University, journal of science, **23(4)**, 435-443.

Khallaf, H., Chai, G., Lupan, O., Chow, L., Heinrich, H., Park, L., and Schult, A. (2009). In-situ boron doping of chemical-bath deposited CdS thin films. *Journal of Physica. Status Solidi A*, **206**, 256–262.

Lawrence, F.J., Botten, L.C., Dossou, K.B. and Sterke C.M. (2008). Antireflection Coatings for two Dimensional Photonic Crystals using Rigorous Impedance Definition. *Applied Physics letters*, **93**, 1-3.

Maissel, L.I. and Glang, R. (1970). *Hand book of thin film Technology*. McGraw Hill: New York.

Marko, J. and Marko, T. (2014). Efficiency limits in photovoltaics- case of single junction solar cells. *Facta Universitatis: Electronics and Energetics*, **27**, 631- 638.

Markvart, T. (1998). *Solar Electricity*. John Wiley and Sons. New York.

Markvart, T. (2000). Light harvesting for quantum solar energy conversion: *Progress in Quantum Electronics*, **24**, 107.

Misle, T. (2009). *Shunt passivation process for CdTe solar cell -New Post deposition technique*. (Msc.-Thesis), University of Toledo. Toledo.

Modaffer, A. M., Mousa, A.M. and Ponpon, J.P. (2009). Optical and optoelectronic properties of PbCdS ternary thin films deposited CBD. *Journal of Semiconductor Technology and Science*. **9(2)**, 1-6.

Mohamed, R. M., AbdelRassoul, R. A. and Rassoul, E. M. (2007). *Properties of II-VI semiconductor thin films prepared by vacuum evaporation for photovoltaic application. In the proceeding of a Seminar paper, 4th National Radio Science conference (NRSC), Mansoura University, Egypt*.

Mosiori, C.O. (2012). *Electrical and optical characterization of $CdxZn_{1-x}S$ and PbS thin films for photovoltaic applications*. (Master's thesis). Kenyatta University. Kenyatta University Press.

Mulder, B.J. (2006). Optical properties of an unusual form of thin chalcosite (Cu_2S) crystals. *Physica Status Solidi*, **15**, 409-413.

Nair, M. T. S., and Nair, P. K. (1989).Chemical Bath Deposition of Cu_xS Thin Films and Their Prospective Large Area Applications.*Semiconductor Science Technology*,**4**, 191-199.

Nault, R. M. (2005).*Basic research needs for solar energy utilization.* In the proceeding of a seminar on the basic energy sciences workshop on solar energy utilization.Argonne National Laboratory. 3 – 10

Nnabuchi, Mishack, N., Chinedu and Ekuma, E. (2010).*Synthesis and Characterisation of Chemical Bath Deposited CdCoS thin film.**Chalcogenide Letters*, **7**, 31-38.

Oloomi, S. A. A., Saboonchi, A., and Sedaghat, A. (2010).Effects of thin film thickness on emittance, reflectance and transmittance of nano scale multilayers.*International Journal of Physical Science*, **5**, 465–469.

Omar, M. (1975).*Elementary solid state physics.* Wisleyand Sons: New York.

Osoro, O.E. (2011).*Characterization of $\text{Cu}_x\text{O}_y\text{-ZnO:Sn}$ P-N Junction for Solar Cell applications.*(Master's Thesis).Department of Physics.Kenyatta University.

Parreira, P., Lavareda,G. Valente, J., Nunes, F.T., Amaral, A., Nunes, C. (2010). Optoelectronic properties of transparent p-type semiconductor Cu_xS thin films.*Physica Status Solidi*,**207**, 1652-1654.

Pathan, H. M. and Lokhande, C. D. (2003). Deposition of metal chalcogenide thin films by successive ionic layer adsorption and reaction (SILAR) method. *Indian Academy of Sciences*,**27**, 85-111.

Pathan, H. M., Desai, J. D., and Lokhande, C. D. (2002).Modified chemical deposition and physico-chemical properties of copper sulphide (Cu_2S) thin films.*Applied Surface Science*, **202**(1), 47–56.

Philipps, S. (2015).*Progress in Photovoltaics: Research and Applications*, 1993-2015. Fraunhofer: Institute of solar cell energy.

Philips, S.F. (2015). Progress in Photovoltaics: 1993-2015: John WileyandSons. New York.

Philips J.E., Titus J. and Hofmann D. (1997).*Determining the voltage dependence of the light generated current in CuInSe_2 based solar cells using I-V measurements made at different light intensities.* 26th IEEE Photovoltaic Specialist Conf., Anaheim.

Raji, P., C., Sanjeeviraja, C. and Ramachandran, C. (2005). Thermal and structural properties of Spray PyrolysedCdS thin film. *Indian Academy of Sciences*, **233**, 233-238.

Ramya, M. and Ganesan, S. (2011).Study of thickness dependent Characteristics of Cu_2S thin films for various applications.*Iranian Journal of Material Science and Engineering*,**8**, 34-40.

Ramya, M. and Ganesan, S. (2012).Annealing Effects on Resistivity Properties of Vacuum Evaporated Cu_2S Thin Films.*International Journal of Pure and Applied Physics*,**3**, 243-249.

Robert, L. Boylestad, D. and Louis N. (2008). *Electronic Devices and Circuit Theory*. (9th Ed.). Prentice Hall: New Jersey.

Saadeldin, M., Soliman, H. S., Ali, H.A.M., and Sawaby, K. (2014). Optical and Electrical Characterizations of Nanoparticle Cu₂S Thin Films. *Chinese Physical Society and IOP Publishing Ltd.* **23**, 0468031 - 0468035.

Saraf, R. (2012). High Efficiency and cost effective Cu₂S/CdS thin-film solar cell. *Journal of Electrical and Electronics Engineering (IOSR-JEEE)*, **2**, 47-51.

Shah, A., Torres, P., Tscharnner, R., Wyrsh, N., and Keppner, H. (1999). Photovoltaic technology: the case for thin-film solar cells. *Science*, **285**(5428), 692–698.

Shadia, J., Ikhmayies, A., Riyad N., Ahmad, B. (2008). Effect of film thickness on the electrical and structural properties of CdS: In thin films. *American Journal of Applied Sciences*, **5**, 1141-1143.

Schroder, K. (1998). *Semiconductor Material and Device Characterization* (2nd Ed.). John Wiley and Sons. New York.

Shinde, M.S., Ahirrao P.B., Patil, I.J. and Patil, R.S. (2012). Thickness dependent electrical and optical properties of nanocrystalline copper sulphide thin films grown by simple chemical route. *Indian Journal of Pure and Applied Physics*, **50**, 657-660.

Singh, R. S. and Bhushan, S. (2008). Photoconductivity and Photoluminescence studies of chemically deposited Cd(S-Se): CdCl₂, Dy films. *Shri Shankaracharya College of Engineering and Technology, Junwani, Bhilai, Durg (C. G)*, **5(12)**, 377-388.

Siu, C. and Kwok, L. (1978). Cu_xS/CdS thin-film solar cells using chemically sprayed CdS films. *Journal of Physics*, **11**: 5-8.

Sze, S.M. (1981). *Physics of Semiconductor Devices*. (2nd ed.). John Wiley and Sons Ltd., New York.

Takanoglu, D., Yilmaz, K., Ozcan, Y. and Karabulut, O. (2015). Structural, Electrical and optical properties of thermally Evaporated CdSe and In Doped CdSe thin films. *Chalcogenide letters*, **12**, 35-42.

Tauc, J. (1974). *Amorphous and liquid semiconductors*. Plenum press: New York.

Theiss, W. (2002). Analysis of optical spectra by computer simulation-from basics to batch mode. *Theiss Hard-Und Software for Optical Spectroscopy: Aachen, Germany*. Retrieved from <http://www.wtheiss.com/download/simulation.pdf>

Thomas, L. (2008). *Electronic Devices: Conventional Current Version*. (8th Ed.), Pearson International Edition.

Ubale, A. U., Choudhari, D. M., Kantale, J. S., Mitkari, V. N., Nikam, M. S., Gawande, W. J. and Patil, P. P. (2011). Synthesis of nanostructured thin films by chemical route at room temperature and investigation of their size dependent physical properties. *Journal of Alloy and Compounds*, **509**, 9249-9254.

Ugwu, I. and Onah, U. (2007). Optical characteristics of chemical bath deposited CdS thin film characteristics within UV, Visible, and NIR radiation. *The Pacific Journal of Science and Technology*, **8**, 155-161.

Vajpeyi, A. (2011). *Digital and Analogue Electronics*. Retrieved November 29, 2016, from <http://www.iitg.ac.in/apvajpeyi/ph218/Tut-1.pdf>.

Wu, Y., Wadia, C., Wanli, M., Sadtler, B. and Alivisatos, A. P. (2008). Synthesis and Photovoltaic Application of Copper(I) Sulfide Nanocrystals. *University of California: California*, **8**, 2551-2555.

Yilmaz, K. (2004). *Investigation of InSe thin film based devices*. (Ph.D thesis). Middle East Technical University. P. 41-60.

Zeman, M. (2003). Introduction to photovoltaic solar energy. Delft University of technology, **2,6**.

Zweibel, K., Hersch, P., (1984). *Basic Photovoltaic Principles and Methods*. Van Nostrand Reinhold: New York.